Journal of Inflammation Research

Dovepress
Taylor & Francis Group

Open Access Full Text Article

ORIGINAL RESEARCH

Anti-Psoriatic Efficacies of Psorogrit and Divya-Taila, in Murine Models of Imiquimod and TPA-Induced Psoriasis-Like Inflammation are Driven by Modulation in IL-17RA/IL-23 and IL-8/TNF-α Signaling Axes

Acharya Balkrishna[1–4], Sonam Sharma[1], Tapan Dey[1], Madhulina Maity[1], Sunil Shukla[1], Ankita Kumari[1], Meenu Tomer[1], Rishabh Dev[1], Sandeep Sinha[1], Anurag Varshney[1,2,5]

[1]Drug Discovery and Development Division, Patanjali Research Foundation, Governed by Patanjali Research Foundation Trust, Haridwar, Uttarakhand, India; [2]Department of Allied and Applied Sciences, University of Patanjali, Patanjali Yog Peeth, Haridwar, Uttarakhand, India; [3]Patanjali Yog Peeth (UK) Trust Kinning Park, Glasgow, UK; [4]Patanjali Yogpeeth Nepal, Budhanilkantha Metropolitan, Kathmandu, Nepal; [5]Special Centre for Systems Medicine, Jawaharlal Nehru University, New Delhi, India

Correspondence: Anurag Varshney, Drug Discovery and Development Division, Patanjali Research Foundation, Governed by Patanjali Research Foundation Trust, Haridwar, Uttarakhand, India, Email anurag@patanjali.res.in

Video abstract

Point your SmartPhone at the code above. If you have a QR code reader the video abstract will appear. Or use: https://youtu.be/NybDXKLRSTA

Aim: Psoriasis is a chronic inflammatory skin disease that occurs among all age groups, irrespective of gender, and consequently it negatively impacts patient's quality of life. Medicines of herbo-mineral origin are being increasingly used for the mitigation of psoriasis, due to the side effects associated with the available treatment options. Present study characterizes the pharmacological efficacy of Psorogrit (PSO) and Divya-Taila (DT) using in vitro and in vivo assays.

Methods: Human keratinocyte (HaCaT) cells stimulated with TNF-α or Imiquimod (IMQ) were used to generate the in vitro models of psoriasis. PSO was further evaluated for modulation of mRNA expression, cytokine levels and NF-κB reporter activity. The in vivo anti-psoriatic activity of the orally given PSO and topically applied DT was assessed in mouse models of IMQ-induced psoriasis-like skin lesions and 12-O-tetradecanoylphorbol-13-acetate (TPA)-induced ear edema. The animals were randomly allocated to the Normal control, Disease control, Clobetasol, PSO and DT groups. Analysis of ear thickness, ear punch weight, spleen weight, histopathology by hematoxylin and eosin (H&E), and *Keratin 17* (*KRT 17*) mRNA expression was measured for evaluation of these herbal formulations. Moreover, the phytochemical composition of PSO and DT was evaluated by UHPLC and GC/MS/MS.

Results: Cytosafe concentrations of PSO significantly attenuated IL-8 release as well as mRNA expressions of *IL-8*, *TNF-α*, and *IL-1β* in TNF-α-induced human skin keratinocytes. PSO was observed to decrease the TNF-α-induced NF-κB reporter activity. Additionally, in IMQ-induced HaCaT cells, PSO reduced the release of IL-17RA and mRNA expression of *IL-23* and *IL-17RA*. In the in vivo IMQ-induced model, PSO and DT were able to ameliorate the IMQ-induced increase in ear punch weight, relative spleen weight, and histopathological changes in both ear and dorsal back skin. In TPA-induced ear edema model, PSO and DT reduced the increase in ear thickness, ear punch weight, and histopathological lesions. Besides, the phytochemical analysis of PSO and DT revealed the presence of phytometabolites known to have anti-inflammatory activities.

Conclusion: The combinatorial use of Psorogrit and Divya-Taila has the potential to ameliorate clinical and pathological manifestations of psoriasis.

Keywords: cytokine, Divya-Taila, imiquimod, IL-17RA, NF-κB, psoriasis, Psorogrit, TPA

Received: 7 November 2024
Accepted: 4 March 2025
Published: 18 April 2025

Introduction

Psoriasis is a chronic inflammatory skin disease characterized by hyperproliferation of keratinocytes, infiltration of immune cells (mostly dendritic and T cells) in the epidermis and dermis, and underlying vascular deformations.[1,2] A complex interplay of genetic, environmental, and immunological co-factors underlies the etiology of psoriasis.[2] A World Health Organization 2016 report, estimated that psoriasis prevalence in countries ranges from 0.09% to 11.4%.[3]

Previously, genetic predisposition was considered the most important factor associated with the higher prevalence of psoriasis among the Caucasians and Scandinavian populations.[4,5] Contemporary studies have deciphered several intracellular signaling pathways, including IL-23/IL-17, NF-κB, MAPK kinase, and the IL-6/JAK/STAT3 axis that play a pivotal role in the pathogenesis of psoriasis.[6,7] Elevated levels of cytokines of the IL-23/IL-17 family were detected in cutaneous lesions and serum of psoriasis patients and are critical for the development of autoimmunity[6,8,9]. Further, IL-17 promotes the release of IL-6, IL-8, GM-CSF, and ICAM-1 in keratinocytes.[9–11] Psoriasis is also considered a comorbid factor for developing psoriatic arthritis, cardiovascular diseases (atherosclerosis), Crohn's disease, and uveitis.[12–14] Over the years there has been significant advancement in understanding the pathogenesis of psoriasis, resulting in the development of disease management strategies. Among the various management strategies, light therapy and topical application of corticosteroids, vitamin D analogs, retinoids, and calcineurin inhibitors remain the mainstay for the therapeutic management of psoriasis.[15–18] However, these approaches are associated with various adverse effects on the patients which limits their use for long-term therapy.[19] The use of corticosteroids topically has risk of skin atrophy and infections while systemic absorption could lead to development of Cushing syndrome, osteonecrosis, retardation of children's growth as well as suppression of adrenal gland.[20,21] The treatment choice for psoriasis depends upon the location, severity of comorbidities, and patient's preferences. Over the past years, biologicals have emerged as prominent therapeutics for psoriasis.[22] Compared to conventional therapies, biological therapies have a selective targeted approach and, therefore, can be useful for the long-term treatment of psoriasis.[23] The use of biologicals like TNF-α, IL-17, IL-23, and IL-12/23 antibodies are known to regulate the extracellular pathways[23] and modulate the immune system, which is beneficial in controlling psoriasis-associated inflammation.[22] Despite their significant effectiveness, there are several challenges and limitations of these medications, including primary and secondary treatment failures.[24] The high cost of these medications further limits their use in lower-middle income countries.[25] Thus, recently the focus has been shifted towards the development of herbal formulations for the mitigation of psoriasis.[26] Natural compounds demonstrated anti-inflammatory activities and may serve as an attractive option to mitigate psoriasis due to their multifaceted effects, safety, and cost-effectiveness.[19,27–30] Plants like *Tinospora cordifolia* (Giloy), *Berberis aristata* (Daruhaldi), *Cassia fistula* (Amaltas), *Hippophae rhamnoides* (Seabuckthorn), *Curcuma longa* (Haldi), *Azadirachta indica* (Neem), *Sesamum indicum* (Sesame), *Withania somnifera* (Ashwagandha), and *Caesalpinia bonducella* (Karanj) have been utilized for skin related diseases since ancient times.[31–34] In the current study, the efficacy of a plant-based formulation, Psorogrit (PSO) was tested in the in vitro model of TNF-α or IMQ-induced inflammation in differentiated human keratinocytes (HaCaT cells). In addition, Divya-Taila, which is a plant-based topical formulation, was evaluated along with PSO to determine their combinatorial effects against psoriasis using two different in vivo mice models, namely IMQ-induced psoriatic skin model and the 12-O-Tetradecanoylphorbol-13-acetate (TPA)-induced ear edema model.

Materials and Methods

Reagents

Psorogrit (PSO) (Internal Batch # PRFT/CHIN/0522/0326) and Divya-Taila (DT) (Internal Batch # PRFT/CHIN/0422/0286) were sourced from Divya Pharmacy, Haridwar, India. The composition of PSO and DT is defined in Tables 1 and 2, respectively. 0.05% Clobetasol Propionate IP (Tenovate Cream, GSK Ltd, India, Batch no: EL968) was locally procured. Human recombinant TNF-α (Cat. No. 300–01A) was purchased from PeproTech, USA. Imiquimod (Cat. No. 10747) for in vitro experiments was procured from TCI, India. The reference standard compounds Magnoflorine (ChemFaces, China), Protocatechuic acid (Natural remedies, India), Methyl gallate (TCI, India), Cinnamic acid (SRL, India) Gallic acid (Loba Chemie, India); and Vanillic acid, Rutin, Palmatine hydrochloride, Berberine chloride and β-Ecdysone were purchased from Sigma Aldrich, USA. The cell culture media Dulbecco's modified Eagle's medium (Gibco), Fetal Bovine Serum (Cat No.

Table 1 Herbal Composition of Psorogrit Tablets (Each- 540 mg)

Scientific name	Sanskrit Binomial name	Vernacular name	Parts	Reference Book	Page No.	Quantity (mg/tablet)
Dry extracts of						
Azadirachta indica A. Juss.	Picumardakaḥ nimbaḥ (पचिुमर्दकः नम्बिः)	Neem	Leaf	B.P.N.	314–315	100
Tinospora cordifolia (Willd.) Hook.f. and Thomson	Saptaśirikā aromapatrā (सप्तशरिका अरोमपत्रा)	Giloy	Stem	B.P.N.	257–259	100
Cassia fistula L.	Hemapuṣpakam kṛtamālyam (हेमपुष्पकम् कृतमाल्यम्)	Amaltas	Fruit	B.P.N.	66–67	100
Albizzia lebbeck (L.) Benth.	Mṛdusumakam śirīṣam (मृदुसुमकम् शरिीषम्)	Siras	Bark	B.P.N.	506–507	50
Moringa pterygosperma Gaertn;Syn.-*Moringa oleifera* Lam.	Śigrukaḥ sitapuṣpaḥ (शगि्रुकः सतिपुष्पः)	Sahijan	Leaf	A.P.I.-Part I, Vol- II	161	30
Cyperus scariosus R.Br.	Jalamuk nāgaramustakaḥ (जलमुक् नागरमुस्तकः)	Nagarmotha	Rhizome	B.P.N.	233–234	20
Caesalpinia bonducella (L.) Fleming; Syn.- *Guilandina bonduc* L.	Ṛjuprakaṇṭaḥ prakaṇṭiśimbaḥ (ऋजुप्रकण्टः प्रकण्टशिम्बिः)	Karanj	Seed	B.P.N.	336–338	40
Holarrhena antidysenterica (G.Don) Wall. ex A.DC.; Syn.-*Holarrhena pubescens* Wall ex G.Don	Kuṭajakaḥ yavaphalaḥ (कुटजकः यवफलः)	Indrajau	Seed	B.P.N.	73–74	20
Berberis aristata DC.	Pītadrukaḥ haridruḥ (पीतद्रुकः हरदि्रुः)	Daruhaldi	Whole plant	B.P.N.	115–116	20
Fine Powder of						
Ras Manikya		Classical Preparation	-	A.F.I-I	270	20

Notes: Excipients used per tablet of Psorogrit include *Acacia arabica* (8 mg), Hydrated Magnesium Silicate (8 mg), Microcrystalline cellulose (16 mg), and Sodium carboxymethyl cellulose (8 mg).
Abbreviations: B.P.N., Bhavprakash Nighantu Edition –2010; I.P., Indian Pharmacopoeia – 2014; A.F.I.- I, The Ayurvedic Formulary of India-Part-I-Second Revised Edition; A.P.I-Part I, Vol-II, The Ayurvedic Pharmacopoeia of India- Part-I, Vol-II.

Table 2 Herbal Composition of Divya-Taila (per 100 gm)

Scientific Name	Sanskrit Binomial Name	Vernacular Name	Parts	Reference Book	Page No.	Quantity (gm/100 gm)
Withania somnifera (L.) Dunal	Aśvagandhakaḥ svāpakaraḥ (अश्वगन्धकः स्वापकरः)	Ashwagandha	Seed	B.P.N.	379–380	12
Hippophae rhamnoides L.	Amlāṭakaḥ cukraḥ (अम्लाटकः चुक्रः)	Seabuckthorn	Seed	B.P.N.	587	13
Berberis aristata DC.	Pītadrukaḥ haridruḥ (पीतद्रुकः हरदि्रुः)	Daruhaldi	Stem/Rt. wood	B.P.N.	115–116	20
Curcuma longa L.	Haridrakā pītarāgā (हरदि्रका पीतरागा)	Haldi	Rhizome	B.P.N.	111–112	15
Azadirachta indica A. Juss.	Picumardakaḥ nimbaḥ (पचिुमर्दकः नम्बिः)	Neem	Seed	B.P.N.	314–315	20
Sesamum indicum L.	Tilakam romanālam (तलिकम् रोमनालम्)	Sesame	Seed	A.P.I.-Part-I, Vol.-6	224	20

Abbreviations: B.P.N., Bhavprakash Nighantu Edition –2010; A.P.I-Part I, Vol-6, The Ayurvedic Pharmacopoeia of India- Part-I, Vol-6.

RM9955, HiMedia, India), and keratinocyte-SFM media (KSFM) (Gibco) were used for the in vitro study. The animal feed diet (18% Protein-5L79, HSN No. 2309901) was purchased from Hylasco Biotechnology, India. 12-O-tetradecanoylphorbol-13-Acetate (TPA) (Cat No. 79346) was purchased from Sigma Aldrich, USA. Imiquimod (Imiquad, Glenmark

Pharmaceuticals, India) was purchased locally. For depilation, Veet hair removal cream (Reckitt Benckiser, United Kingdom) was purchased locally. HPLC grade acetonitrile (Cat. No. 40030LC250) was procured from Finar (Gujarat, India), methanol (Cat. No. M0275) from Rankem (Maharashtra, India), orthophosphoric acid AR grade (Cat. No. O0050) from Rankem (Maharashtra, India) and diethylamine AR grade (Cat. No. D0100) from Rankem (Maharashtra, India).

Phytochemical Analysis of Psorogrit

500 mg of powdered Psorogrit tablet was transferred to a 10 mL volumetric flask and 7 mL of methanol: water (80:20) was added and sonicated for 30 min. This solution was centrifuged, cooled and diluted with the same diluent to the volume. The solution was then centrifuged at 5000 rpm for 5 min and filtered by a 0.45 µm nylon filter. The filtered solution was further used for its phytochemical analysis.

Stock solutions of gallic acid (Potency 100.47% w/w, Loba Chemie, Cat. No. 3910), magnoflorine (Potency 98.0% w/w, Chem faces, Cat. No. CFN98071), protocatechuic acid (Potency 99.5% w/w, Natural remedies, Cat. No. P006), methyl gallate (Potency 99.9% w/w, TCI, Cat. No. G0017), vanillic acid (Potency 98.2% w/w, Sigma Aldrich, Cat. No. 68654), rutin (Potency 94.20% w/w, Sigma Aldrich, Cat. No. 78095), cinnamic acid (Potency 99.7% w/w, SRL, Cat. No. 29955), palmatine hydrochloride (Potency 96.9% w/w, Sigma Aldrich, Cat. No.361615), berberine chloride (Potency 88.4% w/w, Sigma Aldrich, Cat. No. PHR1502) and β-ecdysone (Potency 99.9%w/w, PHY- proof, Cat. No. 89651) (1000 µg/mL) were prepared by dissolving accurately weighed standards in methanol individually. 0.05 mL of each standard was mixed and diluted to 1 mL to prepare a 50 µg/mL concentration of standard mix working solution.

The quantification of marker compounds was performed by Prominence-XR UHPLC system (Shimadzu, Japan) equipped with a Quaternary pump (NexeraXR LC-20AD XR), DAD detector (SPD-M20 A), Auto-sampler (Nexera XR SIL-20 AC XR), Degassing unit (DGU-20A 5R) and Column oven (CTO-10 AS VP). The elution was carried out at a 1.0 mL/min flow rate using a gradient elution of mobile phase A (0.1% orthophosphoric acid in water, v/v; adjust pH 2.5 by diethylamine and mobile Phase B (Acetonitrile). This experiment was performed on a Shodex C18-4E (4.6 × 250 mm, 5 µm) column. Gradient programming of the solvent system for mobile phase B was set as 5 to 10% for 0 to 5 min, 10 to 12% from 5 to 10 min, 12% from 10 to 20 min, 12 to 30% from 20 to 40 min, 30 to 45% from 40 to 50 min, 45 to 70% from 50 to 60 min, 70 to 80% from 60 to 65 min, 80 to 5% from 65 to 66 min and 5% from 66 to 70 min. 10 µL of standard and test solution were injected and column temperature was maintained at 35 °C. Wavelengths were set at 270 nm for gallic acid, magnoflorine, protocatechuic acid, methyl gallate, vanillic acid, rutin, cinnamic acid, berberine, and palmatine and 247 nm for β-ecdysone.

Chemical Characterization of Divya-Taila

For fatty acid methyl ester (FAME) analysis, DT (100 mg) was mixed with 0.4 N methanolic sodium hydroxide (NaOH) and refluxed at 60 °C for 5 min. The whole mixture was then mixed with 14% methanolic boron trifluoride (BF_3) and refluxed for 2 min, followed by the addition of 4 mL n-heptane and refluxed for another 1 min. The solution was cooled at room temperature and then 15 mL of saturated sodium chloride solution was added and transferred into a separating funnel. The supernatant (n-heptane layer) was passed through the anhydrous sodium sulphate and collected in a glass vial. This solution was diluted further 50 times with n-heptane. The resulting solution was injected into the GC/MS/MS system (Agilent Technologies 7000D GC/MS Triple Quad, USA). The quantification of Palmitic acid, Palmitoleic acid, Stearic acid, Oleic acid, and Linoleic acid was done based on standards as % w/w.

Cell-Based Assessment of PSO

Immortalized human skin keratinocyte cell line (HaCaT) was procured from Krishgen Biosystems, USA (Cat. No. KCC0090). The reporter cell line THP1-Blue NF-κB was obtained from InvivoGen, USA (Cat. No. thp-nfkb). HaCaT cells were cultured in Dulbecco's modified Eagle's medium with heat-inactivated 10% Fetal Bovine Serum (FBS). THP1 cells were cultured in RPMI 1640 media supplemented with 10% FBS and antibiotics as per the manufacturer's instructions. The cells were maintained at 37 °C and 5% CO_2 in a humidified incubator. The schematic representation of the in vitro experiments using differentiated HaCaT cells is summarized in Figure 1. Briefly, HaCaT cells were seeded in keratinocyte-

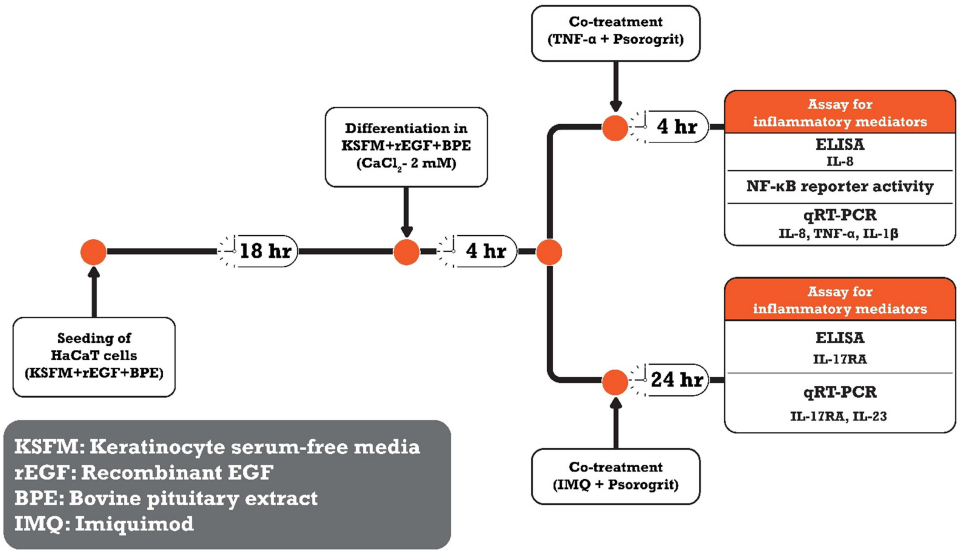

Figure 1 Schematic representation of the in vitro experiments showing differentiation of human skin keratinocytes (HaCaT) followed by TNF-α or IMQ-induced inflammation and treatment with Psorogrit.

SFM media (KSFM) with the addition of supplements, recombinant epidermal growth factor (rEGF; 0.2 ng/mL), and bovine pituitary extract (BPE; 30 µg/mL). For differentiation, 2 mm calcium chloride ($CaCl_2$) was added to the HaCaT cells, and cells were incubated for 4 hr. These differentiated HaCaT cells were further utilized for the experiments.[35] In one of the psoriasis models, human recombinant TNF-α was used as an inflammatory stimulus at a concentration of 10 ng/mL for cytokine release and gene expression studies. To determine the cytosafe doses of PSO (1–100 µg/mL) in differentiated HaCaT cells, cell viability analysis was conducted by Alamar blue reduction assay. The fluorescence intensity was measured at Ex/Em- 560/590 nm in an Envision (Perkin Elmer, USA) multimode plate reader. The cell supernatant of these experiments was collected for quantification of the IL-8 level. ELISA for IL-8 was performed using a Human IL-8 ELISA kit (Cat. No. 555244, BD Biosciences, USA) as per the manufacturer's instructions. Data were represented as mean ± SEM (n = 3). Furthermore, mRNA expression of pro-inflammatory mediators *TNF-α*, *IL-1β*, and *IL-8* was studied. For evaluating nuclear factor kappa B (NF-κB activity), reporter cell line THP1-Blue NF-κB cells were used. Briefly, 5×10^5 cells/mL were seeded in a 96-well plate and co-treated with TNF-α (10 ng/mL) and Psorogrit (10, 30, and 100 µg/mL) for 24 hr. For evaluating the NF-κB activity, the secreted embryonic alkaline phosphatase (SEAP) was measured in cell supernatants, as per the manufacturer's instruction. The optical density was read at 630 nm using an Envision (Perkin Elmer, USA) multimode plate reader. Another cell-based psoriasis model was developed using imiquimod (IMQ, 100 µM). To determine the levels of released IL-17RA, the differentiated HaCaT cells were co-treated with IMQ (100 µM) and PSO (10, 30, and 100 µg/mL) for 24 hr and ELISA was performed as per the manufacturer's instructions (Cat. No. SEK10895, Sino Biological Inc., China). Data was represented as mean ± SEM (n =3). Furthermore, mRNA expression of *IL-17RA* and *IL-23* was measured in presence of IMQ and PSO.

In vivo Assessment of PSO and DT

Experimental Animals

The present study is being reported as per the ARRIVE guidelines.[36] The Institutional Animal Ethics Committee reviewed the proposed animal experimental protocols. Subsequently, the committee approved these experiments, vide approval number PRIAS/LAF/IAEC-125 for TPA-induced ear edema and approval number PRIAS/LAF/IAEC-126 for imiquimod-induced psoriasis-like skin lesions. All husbandry practices and experimental procedures were conducted under strict accordance with the standards prescribed by the Committee for Control and Supervision of Experiments on Animals (CCSEA), Department of Animal Husbandry and Dairying, Ministry of Fisheries, Animal Husbandry and Dairying, Government of India. The animals were housed under normal conditions: 22 ± 2°C, 55 ± 5% relative humidity,

https://doi.org/10.2147/JIR.S505245

and a 12 hr night/day cycle. They were provided standard feed and water *ad libitum*. During the animal experiments, all efforts were made to minimize suffering. At the end of the experiments, the animals were humanely sacrificed under an overdose of thiopental sodium anesthesia (150 mg/kg), administered intraperitoneally. The experiments were conducted by skilled veterinarians and in vivo pharmacologists possessing the required knowledge and expertise in laboratory animal sciences and medicine.

In vivo Model 1: Imiquimod-Induced Psoriasis-Like Skin Lesions

Experimental Protocol

Thirty-eight male, BALB/c mice, aged five-six weeks were procured from Vivo Bio Tech Ltd., Hyderabad, India (a technology licensee of Taconic Biosciences, USA) were used for an IMQ-induced psoriasis-like skin lesions study. The schematic representation of the IMQ-induced in vivo experimental protocol is summarized in Figure 2. Briefly, after a week of quarantine, animals were randomly allocated into 5 different groups based on their respective body weights and acclimatized to the experimental room for another 5 days. The animals treated with PSO 40 + DT and PSO 400 + DT were prophylactically dosed with PSO at the doses of 40 and 400 mg/kg/day respectively, suspended in 0.5% methylcellulose, as a gavage for 14 days. The animals allocated to the normal control, disease control, and clobetasol groups were orally administered an equal volume of 0.5% methylcellulose. After completion of the prophylactic period, the back skins of all the animals were depilated (2 × 3 cm area) by utilizing Veet hair removal cream. The commercially available, 5% IMQ cream (62.5 mg) was applied topically on the depilated back skin of animals except in the normal control group, for 8 consecutive days. Similarly, IMQ was also applied on the right ear of animals at a dose of 35 mg except in the normal control group, for 8 consecutive days. An equal amount of Petroleum jelly (Vaseline) was applied to the ear and back skin of the normal control group animals. During this disease induction period of 8 days, animals allocated to PSO 40 + DT and PSO 400 + DT groups were orally administered with PSO at the doses of (40 and 400 mpk/day), respectively along with the topical application of DT (Ear- 40 µL/day and Back skin- 200 µL/day), 4 hr after IMQ application, except for the control group. The positive control group was treated with 0.05% clobetasol propionate cream (Ear skin- 20 mg/day; Back skin – 100 mg/day), 4 hr after IMQ application, once daily for the entire 8-day study period. All the animals were monitored twice daily for the duration of a 27-day study period for the presence of any aberrant clinical signs, morbidity, and mortality till terminal sacrifice. On the 9th day, the animals were humanely sacrificed under an overdose of sodium thiopentone anesthesia (150 mg/kg, *i.p*). Moreover, during the planning of the experiment, certain humane endpoints were included in the study to alleviate the severe suffering and distress of the animals. The humane endpoint criteria include severe body weight loss (more than 20%), severe erythema and desquamation of skin along with reduced mobility or immobility, anorexia, vocalization characteristic of pain, and persistent recumbency. However, these aberrant clinical signs were not demonstrated by any of the animals in the current experiment and all the animals were humanely sacrificed at the experimental endpoint.

Measurement of Ear Punch Weight

For measurement of ear punch weight, on the 9th day, animals were humanely sacrificed under the overdose of sodium thiopentone anesthesia (150 mg/kg, *i.p)*. Subsequently, ear punches (two biopsy punches per pinna) were excised from the animals by using a biopsy punch (5 mm). The biopsy punches were then weighed. The percentage inhibition of ear punch weight was calculated by considering the disease control data as 0% and the normal control group as 100% inhibition.

Measurement of Relative Spleen Weight

For measurement of spleen weight, post-sacrifice, the spleen of animals was harvested and weighed. The percentage inhibition of spleen weight was calculated by considering the disease control data as 0% and the control group as 100% inhibition. The relative spleen weight was calculated based on the following formulae:

$$\text{Relative weight of Spleen } (\%) = \frac{\text{Spleen weight (g)}}{\text{Terminal Body weight (g)}} \times 100$$

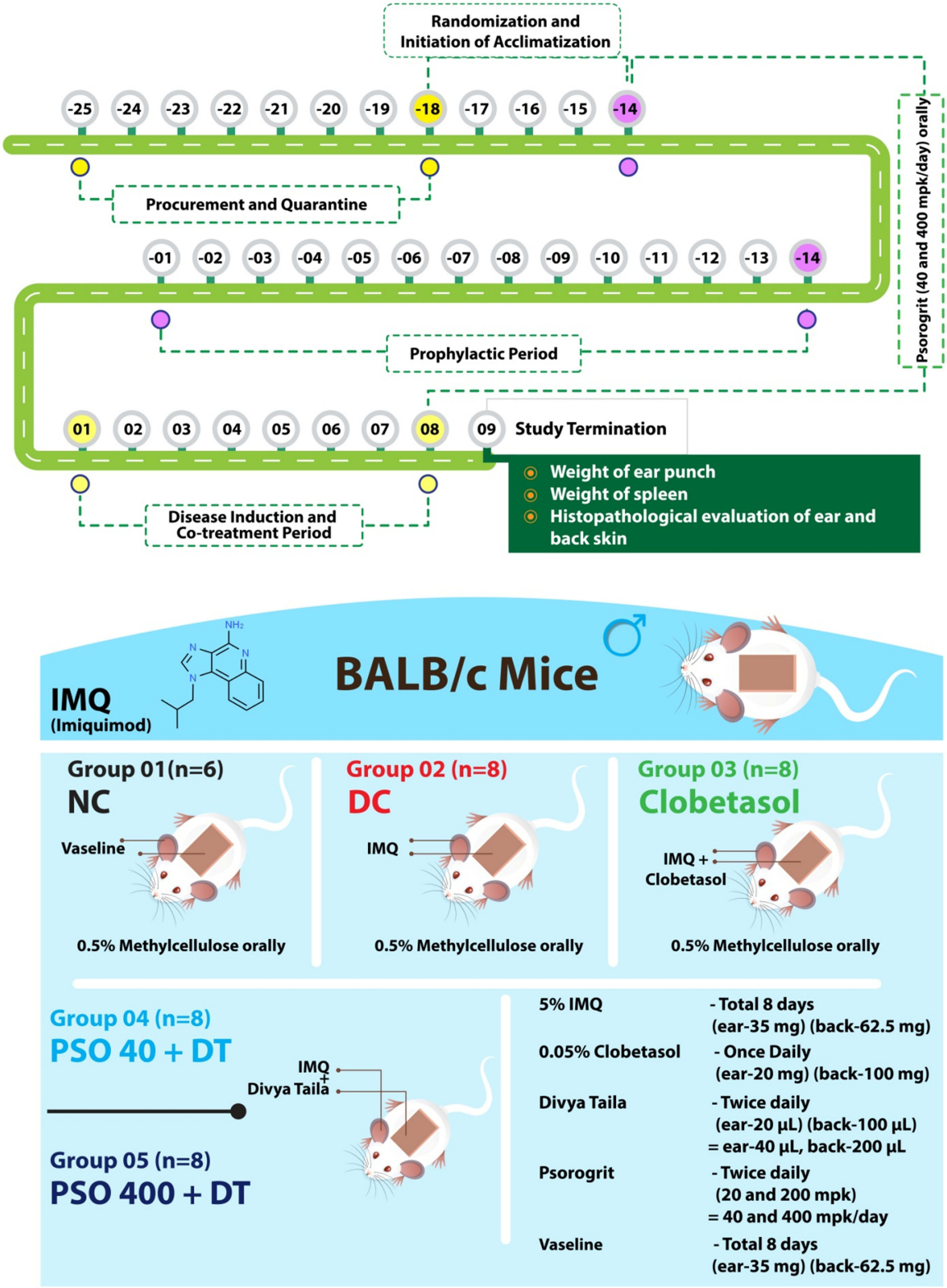

Figure 2 Schematic representation of the IMQ-induced psoriatic skin in vivo experiment.

https://doi.org/10.2147/JIR.S505245

In vivo Model 2: TPA-Induced Ear Edema

Experimental Protocol

Forty-six, male, Swiss Webster mice, aged six to eight weeks, were procured from Vivo Bio Tech Ltd., Hyderabad, India, a Taconic Biosciences licensed, domestic animal supplier and used for TPA-induced ear edema study. The schematic representation of the TPA-induced in vivo experimental protocol is summarized in Figure 3. Briefly, after a week of quarantine, animals were randomly allocated into 6 different groups based on their respective body weights and acclimatized to the experimental room for another 5 days. The doses of PSO were calculated from their human equivalent dose *i.e.* 2 g/day as described elsewhere.[37] The mice grouped as PSO 40 + DT, PSO 120 + DT, and PSO 400 + DT were prophylactically administered with PSO (40, 120, and 400 mpk/day suspended in 0.5% methylcellulose, respectively), as a gavage for 14 days before TPA induction. After completion of the prophylactic dosing period, TPA was applied topically to all animals except those allocated to the control group. For psoriasis induction in mice, 20 µL (Stock: 125 µg/mL) of the TPA (in acetone) solution was applied topically to the right ear, once a day on 6 alternative days (Day-1, 3, 5, 7, 9, and 11). The left ear of the mice was topically applied with 20 µL of acetone. The mice allocated to the control group were topically applied with acetone (20 µL) on both the left and right ears. PSO (40, 120, 400 mpk/day) orally and DT (40 µL/day) topically were applied throughout the 11-day treatment period 4 hr after TPA application. The positive control group was treated with 0.05% Clobetasol propionate (20 mg/day) once daily for the entire 11-day study period. During the 30-day experimental period, all the animals were observed twice daily for the presence of any abnormal clinical signs, morbidity, and mortality till terminal sacrifice. On the 11th day, 6 hr post-TPA application, animals were humanely sacrificed under the overdose of sodium thiopentone anesthesia (150 mg/kg, *i.p*). Besides, certain humane endpoints were identified and incorporated into the study to humanely euthanize the animals before reaching the experimental endpoint to avoid severe suffering and distress. The criteria for a humane endpoint encompass severe body weight loss (more than 20%), reduced mobility or immobility, anorexia, and persistent recumbency. Nevertheless, none of the animals exhibited such severe clinical abnormalities in the current study, and all the animals were humanely sacrificed at the experimental endpoint.

Measurement of Δ Ear Thickness

Ear thickness was measured daily using a Vernier caliper (Mitutoyo) at 4 hr post-TPA application. The caliper was applied to three different parts of the ear namely the upper, middle, and lower regions where the thickness was recorded in millimeters (mm). The (Δ) increase in ear thickness was obtained from the difference in thickness between the TPA-treated right ear and the acetone-treated left ear. To minimize variation, a single investigator performed all measurements throughout the whole experiment. The percentage inhibition of ear thickness was calculated by considering the disease control data as 0% and the control group as 100% inhibition.

Measurement of Δ Ear Punch Weight

Post-sacrifice, ear punches were excised using a biopsy punch (5 mm) from both the pinnae (two biopsy punches per pinna). Each biopsy punch was then weighed. The (Δ) increase in ear weight was obtained from the difference in weight between the TPA-treated right ear and the acetone-treated left ear. The percentage inhibition of ear punch weight was calculated by considering the disease control data as 0% and the control group as 100% inhibition.

Effect of PSO and DT on Histopathological Analysis and Lesion Score

For both IMQ (ear skin and back skin) and TPA-induced (ear skin) in vivo experiments, the preserved excised samples were processed by using a tissue processor (Leica biosystems; Model: TP 1020, India). The samples were then embedded in paraffin wax using an embedding station (Leica biosystems; Model: Histocore Arcadia H-C, India). Subsequently, 3–5 µm sections were cut using a microtome (Leica biosystems; Model: RM 2245, India), and allowed to float in a tissue floatation bath (ThermoFisher Scientific; Model: Tsgp-10, USA). Further, the sections were placed on glass slides, de-paraffinized, and stained with hematoxylin-eosin. The stained sections were then examined using a compound light microscope (AxioScope-A1, Carl Zeiss, Germany) and imaging was performed using Axiovision software. The representative skin tissue sections were microscopically evaluated for epidermal hyperplasia, inflammatory cell influx, and rete ridges formation. Based on the severity, these lesions were assigned as 0 = absent, 1 = mild, 2 = moderate, 3 = severe

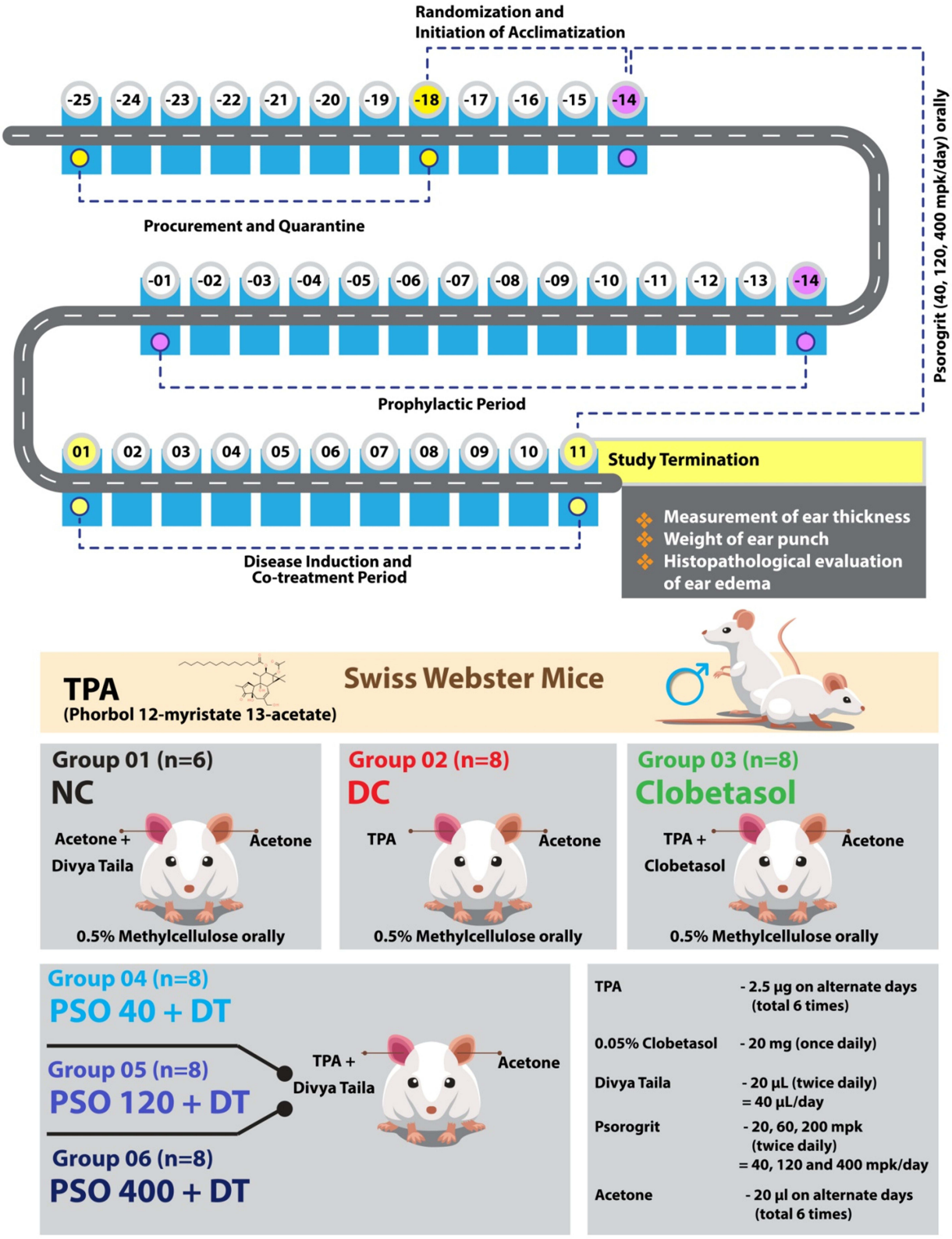

Figure 3 Schematic representation of the TPA-induced ear edema in vivo experiments.

https://doi.org/10.2147/JIR.S505245

and patchy, and 4 = severe and diffuse in distribution. Additionally, the severities of the lesions falling in between two integral scores were assigned an additional value of 0.5. The sum of all these parameter scores was considered the total lesion score. Additionally, the thickness of the epidermis was measured from five random areas using ImageJ software, where the average of the five readings was considered for final statistical analysis.[34,38]

mRNA Expression Analysis

For mRNA expression studies, total RNA was extracted using TRIzol followed by a column-based RNAeasy mini kit (Qiagen, Germany, Cat. no. 74016). Total RNA was then quantified via UV/Vis nano spectrophotometer (NABI, Brussel), and 1µg RNA was then used to synthesize cDNA via Verso cDNA synthesis kit (Thermo Fisher Scientific Inc., MA, USA, Cat. No. AB1453A). Gene expression was studied with PowerUp SYBR Green Master Mix (Applied Biosystems, USA) and run on qTOWER ^{3} G (Analytik Jena, Germany) Real-time PCR system. Data were analyzed using relative fold change ($2^{-\Delta\Delta CT}$) as compared with control using the housekeeping genes (*β-tubulin* or *GAPDH*). The oligonucleotide sequences used for the study include human *IL-8* (F-AGTTTTTGAAGAGGGCTGAGAAT; R-GCTTGAAGTTTCACTGGCATCT), *IL-1β* (F-AAGCTGATGGCCC TAAACAG; R-AGGTGCATCGTGCACATAAG), TNF-α (CCTCCTCTCTGCCATCAAGA; R-CTCACAGGGCAATGA TCCCA), *β-tubulin* (F-GCATCAACTACCAGCCTCCCAC; R-AGGTGCATCGTGCACATAAG), *GAPDH* (F-GGGTGTGAACCACGAGAAAT; R-ACTGTGGTCATGAGCCCTTC), *IL-17RA* (F-AGTTCCACCAGCGATCCAAC; R-GTCTGAGGCAGTCATTGAGGC), *IL-23* (F-GCTTCAAAATCCTTCGCAG; R-TATCTGAGTGCCATCCTTGAG), and murine *KRT 17* (F-GCCCACCTGACTCAGTACAA; R- GGAGCTGAGTCCTTAACGGG), *GAPDH* (F-AAGGTCATCCCAGAGCTG; R-CTGCTTCACCACCTTCTTGA). Data were represented as mean ± SEM (n = 3).

Statistical Analysis

The data were expressed as mean ± standard error of mean (SEM) for each group. Statistical analysis was done using GraphPad Prism 7.4 (GraphPad Software, USA) using one-way ANOVA followed by Dunnett's multiple comparisons post-hoc test. Mean differences and 95% confidence intervals of the mean differences were computed. A $p < 0.05$ value was considered statistically significant.

Results

Phytochemical Analysis of PSO

The quantification of phytochemicals screened by the UHPLC system revealed the presence of Palmatine (1.153 µg/mg), β- Ecdysone (1.009 µg/mg), Berberine (0.552 µg/mg), Protocatechuic acid (0.257 µg/mg), Rutin (0.161 µg/mg), Vanillic acid (0.068 µg/mg), Gallic acid (0.062 µg/mg), Magnoflorine (0.037 µg/mg), Cinnamic acid (0.005 µg/mg) and Methyl gallate (0.004 µg/mg) in PSO (500 mg tablet) (Figure 4).

Chemical Characterization of DT

Based on the reference standards, GC/MS/MS analysis reveals the presence of α-Phellandrene, o-Cymene, Eucalyptol, Terpinolene, α-Curcumene, 7-epi-Sesquithujene, β-Sesquiphellandrene, 1-isobutyl-2,5-dimethylbenzene, (Z)-γ-Atlantone, ar-Turmerone, Tumerone, Curlone, and (E)-Atlantone based on their retention times, in DT (Figure 5A). After quantification, the amount of ar-Turmerone and Eucalyptol was found to be 7.76% and 0.16% w/w in DT. The FAME analysis revealed the presence of Palmitic acid (6.95% w/w), Palmitoleic acid (1.49% w/w), Stearic acid (1.75% w/w), Oleic acid (12.4% w/w), and Linoleic acid (13.29% w/w) in DT (Figure 5B).

PSO Demonstrated Anti-Inflammatory Activity at Cytosafe Concentrations in Differentiated Keratinocyte Cells

PSO was found to be cytosafe upto 100 µg/mL concentration in human keratinocyte cells (Figure 6A). Thus, 100 µg/mL was chosen as the maximum dose for later in vitro experiments. Upon stimulation with TNF-α, differentiated keratinocytes were shown to release a significant amount of neutrophil chemoattractant IL-8 as compared to control cells.

Overlap chromatogram of standard mix (in blue colour) and Psorogrit tablet (PRFT/CHIN/0522/0326) (in pink colour). Gallic acid, Magnoflorine, Protocatechuic acid, Methyl gallate, Vanillic acid, Palmatine, Berberine, Rutin and Cinnamic acid were quantified at 270 nm whereas Beta-Ecdysone was quantified at 247 nm.

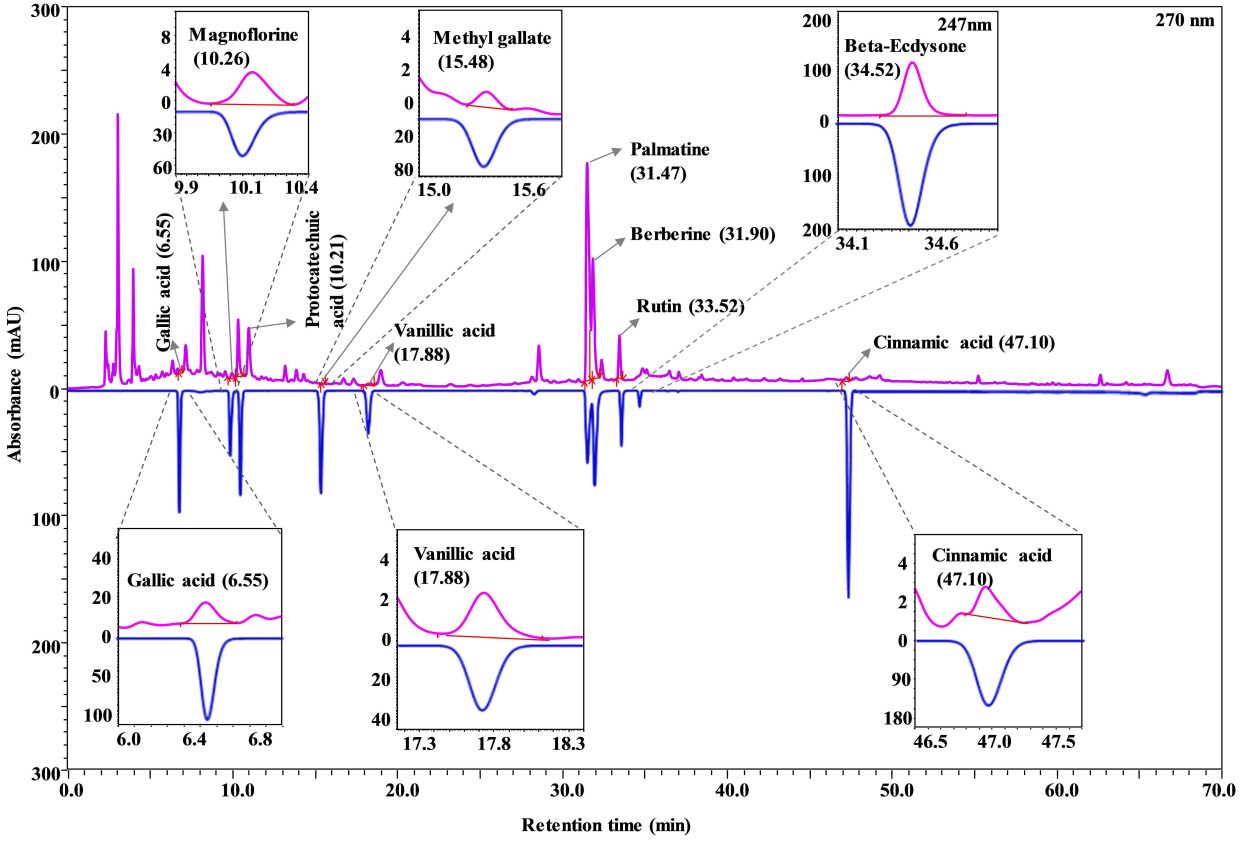

Figure 4 Phytochemical analysis of Psorogrit tablet (PSO) using UHPLC analysis. Overlay chromatogram of the standard mix (in blue colour) and PSO (in pink colour). Gallic acid, Magnoflorine, Protocatechuic acid, Methyl gallate, Vanillic acid, Palmatine, Berberine, Rutin and Cinnamic acid were quantified at 270 nm whereas β-Ecdysone was quantified at 247 nm.

Opposite to that, PSO was found to dose-dependently ($p < 0.01$) downregulate IL-8 release in TNF-α stimulated cells (Figure 6B). Further, the efficacy of PSO was tested on the mRNA expressions of pro-inflammatory mediators *IL-8*, *TNF-α*, and *IL-1β* in TNF-α stimulated keratinocytes. TNF-α- induced cells showed a significant ($p < 0.01$) increase in the mRNA expressions of *IL-8*, *TNF-α*, and *IL-1β* genes as compared to control cells (Figure 6C–E). PSO ($p < 0.01$) dose-dependently reduced the elevated mRNA expressions of the tested genes. The maximum inhibition at the gene expression level was observed at 100 µg/mL of PSO.

As PSO attenuated IL-8 release and mitigated the elevated gene expression of pro-inflammatory mediators, it was thought that PSO might be showing its anti-inflammatory efficacy by regulating the ubiquitous transcription factor NF-κB. Thus, the efficacy of PSO in regulating NF-κB activity was studied using a THP1-Blue-NF-κB reporter cell line. Upon stimulation with TNF-α, NF-κB reporter cells were shown to significantly induce a higher amount of secreted embryonic alkaline phosphatase (SEAP) level (Figure 6F). Though PSO was shown to reduce the SEAP release in TNF-α treated cells, it only showed to be statistically significant ($p < 0.05$) at the highest dose of PSO. Combining all, PSO was shown to effectively mitigate the TNF-α induced inflammatory responses in human keratinocytes.

Further, differentiated keratinocytes were stimulated with IMQ (100 µM), wherein a significant ($p < 0.01$) release of interleukin 17 receptor (IL-17RA) was observed as compared to control cells. On the other hand, PSO was found to significantly reduce IL-17RA release dose-dependently ($p < 0.01$) (Figure 7A). Furthermore, the effects of PSO were assessed on the mRNA expressions of IMQ-induced pro-inflammatory mediators, namely, *IL-17RA* and *IL-23*. IMQ-induced cells displayed a significant ($p < 0.01$) increase in the mRNA expressions of *IL-17RA* and *IL-23* genes which was

https://doi.org/10.2147/JIR.S505245

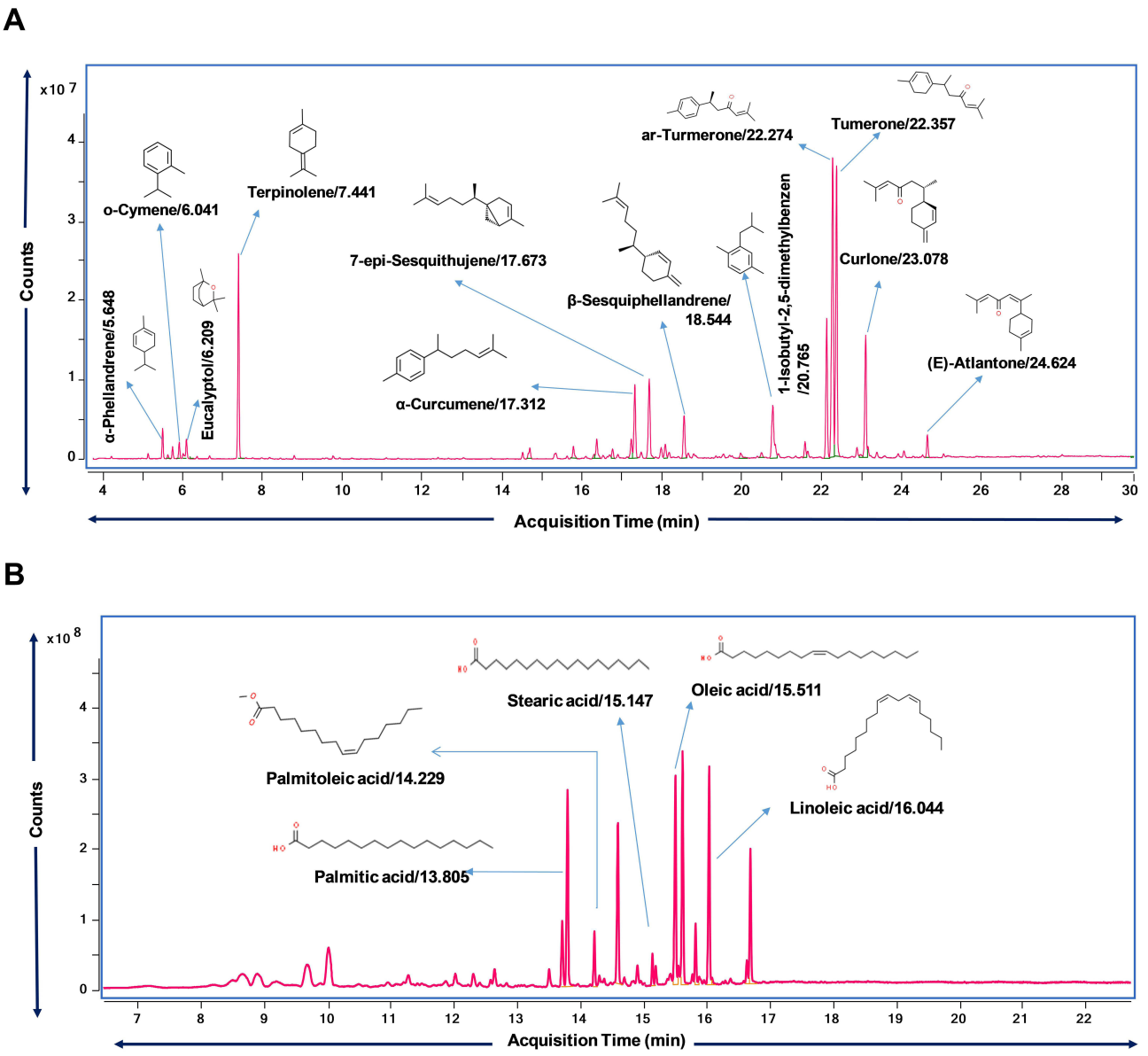

Figure 5 Fatty acid analysis of Divya-Taila (DT) using GC/MS/MS analysis. (**A**) The chromatogram represents the phytochemicals present in DT. (**B**) The chromatogram represents the fatty acid contents of DT. The retention time of individual compounds was mentioned along with compounds.

normalized upon treatment with PSO in a dose-dependent manner (Figure 7B and C). In order to further substantiate these findings, the murine model of IMQ-induced psoriasis-like skin lesions was employed.

In vivo Anti-Psoriatic Activity of PSO and DT

In vivo Model 1: PSO and DT Attenuated IMQ-Induced Ear Biopsy Weight

Here, we first evaluated the weight of ear punches of IMQ-induced tested animals post-sacrifice on Day 9 (Figure 8A). The ear biopsy weight data of the disease control group revealed that IMQ significantly increased the ear punch weight as compared to the normal control group animals. However, PSO 40 + DT and PSO 400 + DT groups demonstrated a dose-dependent decrease in the ear punch weight with the percent inhibition of 51% and 60% ($p < 0.01$), respectively (Figure 8A), when compared with the disease control group. The clobetasol-treated group showed inhibition of 107% as compared to the disease control group.

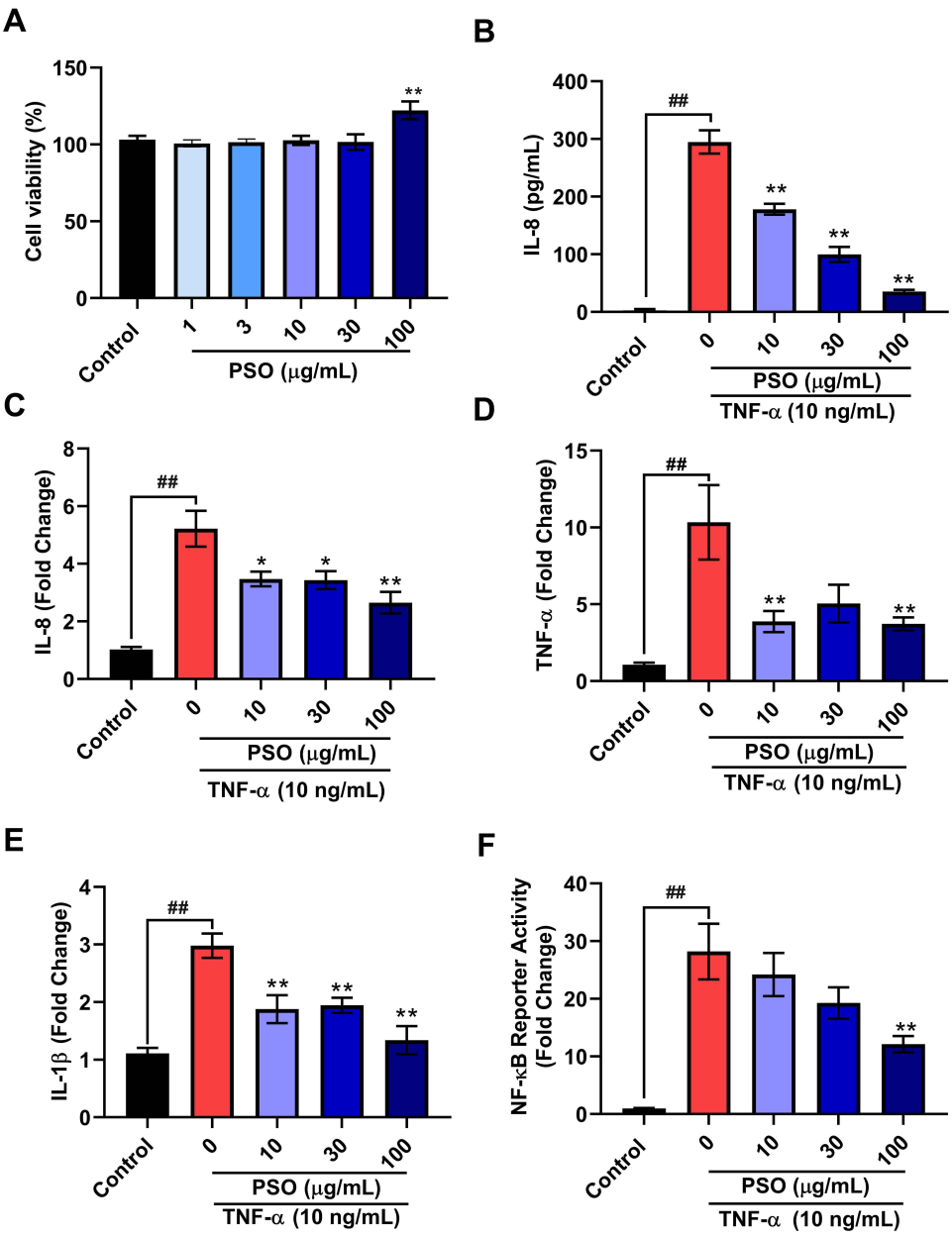

Figure 6 PSO exhibited anti–inflammatory activity in TNF-α induced HaCaT cells. (**A**) The bar chart represents the % cell viability of differentiated HaCaT cells. (**B**) The bar chart represents the IL-8 level in cell supernatants collected from the differentiated cells treated with TNF- α and PSO. (**C**–**E**) The bar chart showing the *IL-8*, *TNF-α*, and *IL-1β* gene expression in HaCaT cells co-treated with PSO and TNF-α. (**F**) The bar chart represents NF-κB activity upon stimulation with TNF-α in the presence of PSO. All values are represented as mean ± SEM, $n = 3$. The statistical significance of the observed differences in the means compared to the PSO (0 µg/mL) was analyzed through one-way ANOVA followed by Dunnett's multiple comparison tests. Statistical significance between Control and PSO (0 µg/mL) group is represented as $^{\#\#}(p < 0.01)$ and between PSO (0 µg/mL) and other PSO (10, 30, 100 µg/mL) groups as $*(p < 0.05)$ or $**(p < 0.01)$.

PSO and DT Reduced IMQ-Induced Relative Spleen Weight

Topical application of IMQ on the skin may lead to systemic inflammation causing an abnormal increase in spleen weight (splenomegaly). Increased infiltration of neutrophils, proerythroblasts, and B cells in the spleen is considered to be the causal factor for splenomegaly due to IMQ application.[39,40] In this study, the relative weight of the spleen was found to be significantly increased in the animals allocated to the disease control group as compared to the normal control group animals (Figure 8B). However, the PSO and DT-treated groups restored the IMQ-induced increase in the relative weight of the spleen ($p < 0.01$) (Figure 8B).

https://doi.org/10.2147/JIR.S505245

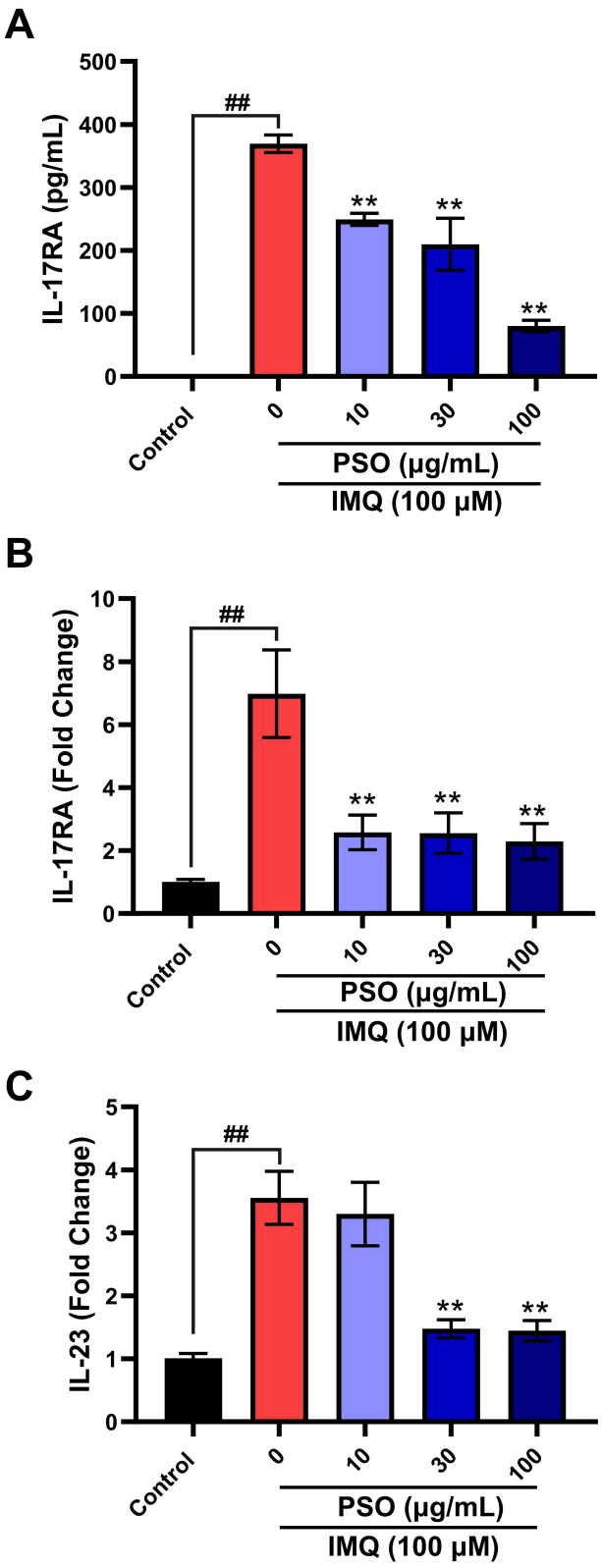

Figure 7 PSO exhibited anti-inflammatory activity in IMQ-induced HaCaT cells. (**A**) The bar chart represents the IL-17RA levels in cell supernatants collected from the differentiated cells treated with IMQ and PSO. (**B** and **C**) The bar chart shows the *IL-17RA* and *IL-23* gene expression in HaCaT cells co-treated with PSO and IMQ. Statistical significance between Control and PSO (0 µg/mL) group is represented as $^{\#\#}(p < 0.01)$ and between PSO (0 µg/mL) and other PSO (10, 30, 100 µg/mL) group $^{**}(p < 0.01)$.

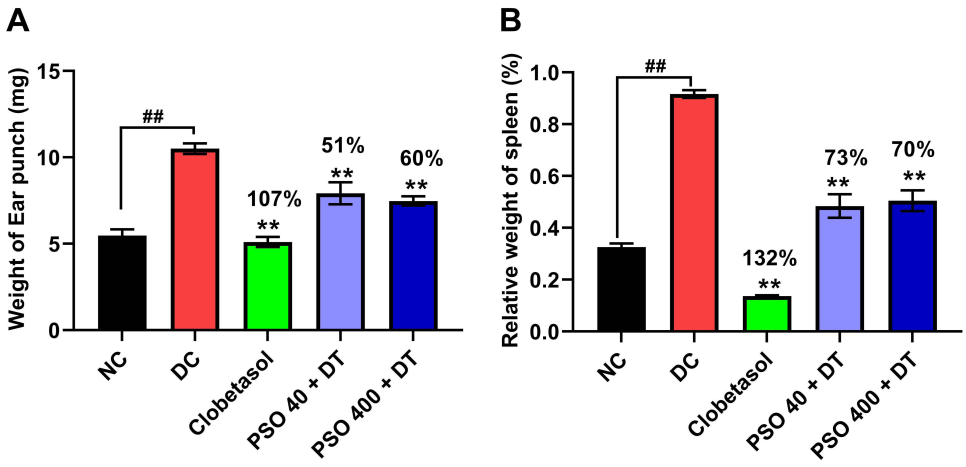

Figure 8 PSO and DT showed anti-psoriatic activity in the IMQ-induced psoriatic model. The bar chart represents (**A**) ear punch weight and (**B**) relative spleen weight in IMQ-induced animals. All statistical analysis was performed using a one-way ANOVA method followed by Dunnett's multiple comparison t-tests (n = 6–8 animals). Statistical significance between NC and DC groups is represented as $^{\#\#}(p < 0.01)$ and between DC and PSO + DT groups (40, 120, and 400 mpk/day) $^{**}(p < 0.01)$.

PSO and DT Mitigated IMQ-Induced Histopathological Changes, Lesion Scores, and *Keratin 17* (*KRT 17*) Gene Expression in Ear Skin Sections

H&E staining of IMQ-stimulated ear skin sections of the disease control animals revealed a strong inflammatory response demonstrated by epidermal hyperplasia, dermal inflammation, and elongated rete ridge formation as compared to the normal control group (Figure 9A I and II). Clobetasol treatment completely abrogated the IMQ-induced microscopic changes in the skin (Figure 9A III). The PSO 40 + DT and PSO 400 + DT groups were shown to significantly reverse the psoriatic changes such as epidermal hyperplasia and dermal inflammation induced by IMQ in ear tissue sections (Figure 9A IV and V).

Similarly, upon lesion scoring, a significant increase ($p < 0.01$) in epidermal hyperplasia and dermal inflammation was observed in the disease control group when compared to the normal control group (Figure 9B and C). However, the PSO and DT-treated groups significantly reduced epidermal hyperplasia and dermal inflammation compared to the disease control group (Figure 9B and C). In addition, the epidermal thickness measured microscopically through the Image J software revealed a significant decrease in epidermal thickness ($p < 0.05$) in PSO and DT-treated groups as compared to the disease control group (Figure 9D).

The *KRT 17* gene is mostly responsible for the hyperproliferation of keratinocytes (hyperkeratosis). It encompasses an abnormal increase in cell size and protein synthesis.[41] In this study, the *KRT 17* gene expression was found to be up-regulated in the ear skin samples of mice allocated to the disease control group as compared to normal control group animals. When compared to the disease control group, the PSO and DT-treated groups at both the tested doses attenuated ($p < 0.01$) the gene expression of *KRT 17* (Figure 9E). The clobetasol propionate-treated group also attenuated the increase in *KRT 17* expression ($p < 0.01$).

PSO and DT Mitigated IMQ-Induced Histopathological Changes in Dorsal Back Skin

The H&E staining of back skin tissue samples also revealed similar histopathological changes as ear skin tissue samples (Figure 10A I and II). Reference control, clobetasol significantly mitigated these parameters in IMQ-induced epidermal hyperplasia and dermal inflammation (Figure 10A III). The PSO and DT-treated groups demonstrated significantly reduced epidermal hyperplasia and dermal inflammation (Figure 10A IV and V). Upon lesion scoring of the structural changes in the back skin tissue samples, the epidermal hyperplasia and dermal inflammation were found to be attenuated ($p < 0.01$) by PSO and DT treatments (Figure 10B and C). In addition, the PSO and DT-administered groups showed a similar trend in reversing the effect of IMQ on the epidermal thickness, measured microscopically ($p < 0.01$) (Figure 10D).

https://doi.org/10.2147/JIR.S505245

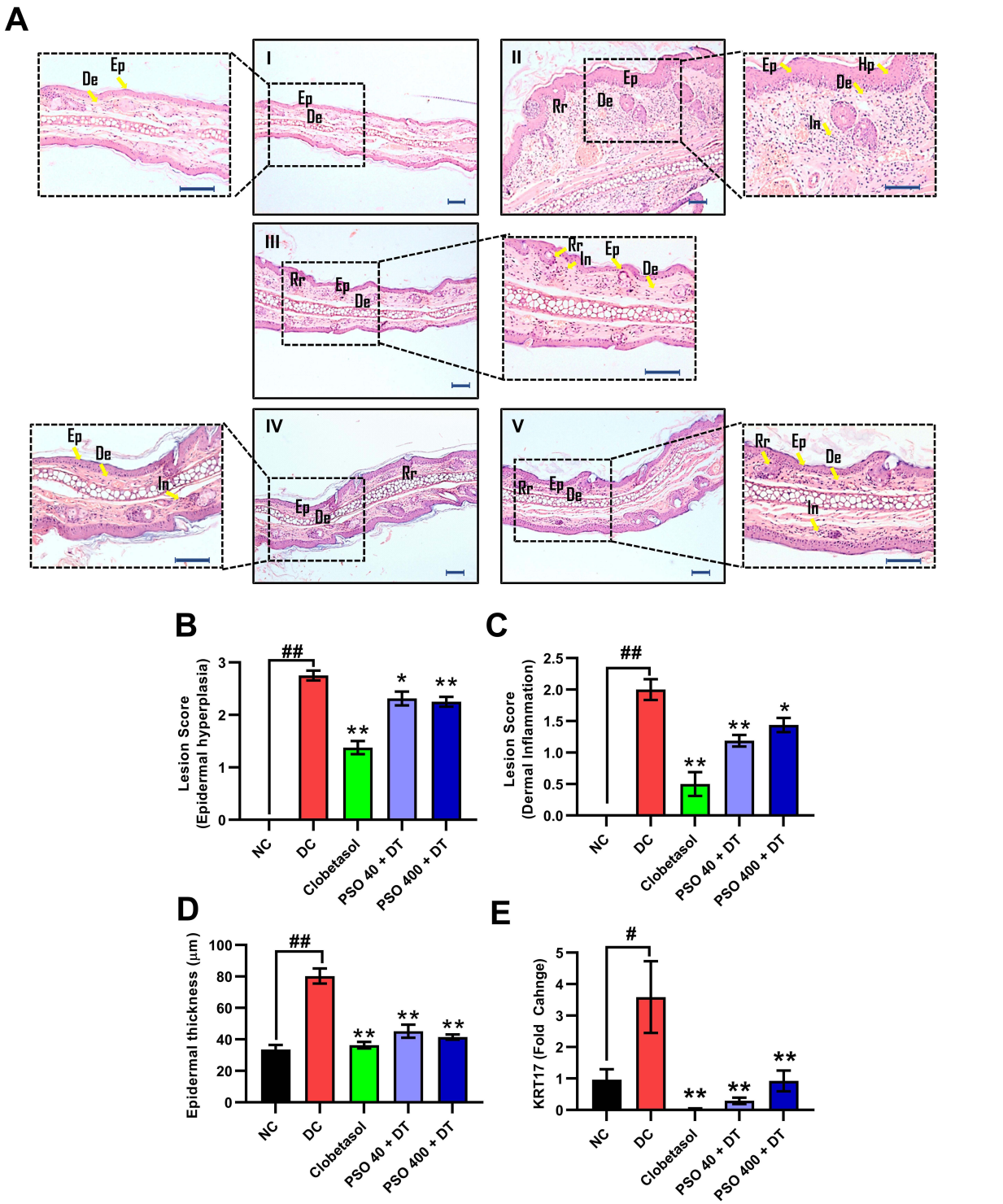

Figure 9 PSO and DT ameliorated histopathological changes and lesion scores of ear skin in IMQ-induced psoriatic model. (**A**) Photomicrographs represent the histopathological analysis of mice ear tissue was performed following hematoxylin and eosin staining. Low-magnification images were obtained at 100X, and the higher-magnification image was obtained at 400X. (I) Normal control (NC): represents normal epidermis (Ep), dermis (De), sebaceous gland (Sg), and cartilage (Ct). (II) Disease control (DC): represents hyperplastic epidermis (Hp), presence of inflammatory cells (In) in the dermis region. (III) IMQ and Clobetasol treated ear: the reduced hyperplastic epidermis (Ep), absence of inflammatory cells in the dermis region. (IV) IMQ and PSO 40 + DT (40 mpk/day PSO and 40 µL/day DT) treated ear: the reduced hyperplastic epidermis (Ep), the reduced presence of inflammatory cells (In) in the dermis region. (V) IMQ and PSO 400 + DT (400 mpk/day PSO and 40 µL/day DT) treated ear: the reduced hyperplastic epidermis (Ep). The scale represents 100 µm (n = 6–8 animals). Yellow arrows depict the specific cellular area of the skin tissue or the characteristic lesion. (**B** and **C**) The bar charts represent lesion scores of epidermal hyperplasia, dermal inflammation, and epidermal thickness of ear skin. (**E**) The bar chart represents changes in *KRT17* gene expression in ear samples. The data were analyzed by one-way ANOVA followed by Dunnett's multiple comparison tests. Statistical significance between NC and DC groups is represented as $^{\#\#}(p < 0.01)$ and between DC and PSO + DT groups (40 and 400 mpk/day) $^{*}(p < 0.05)$ or $^{**}(p < 0.01)$. The scale bar represents 100 µm.

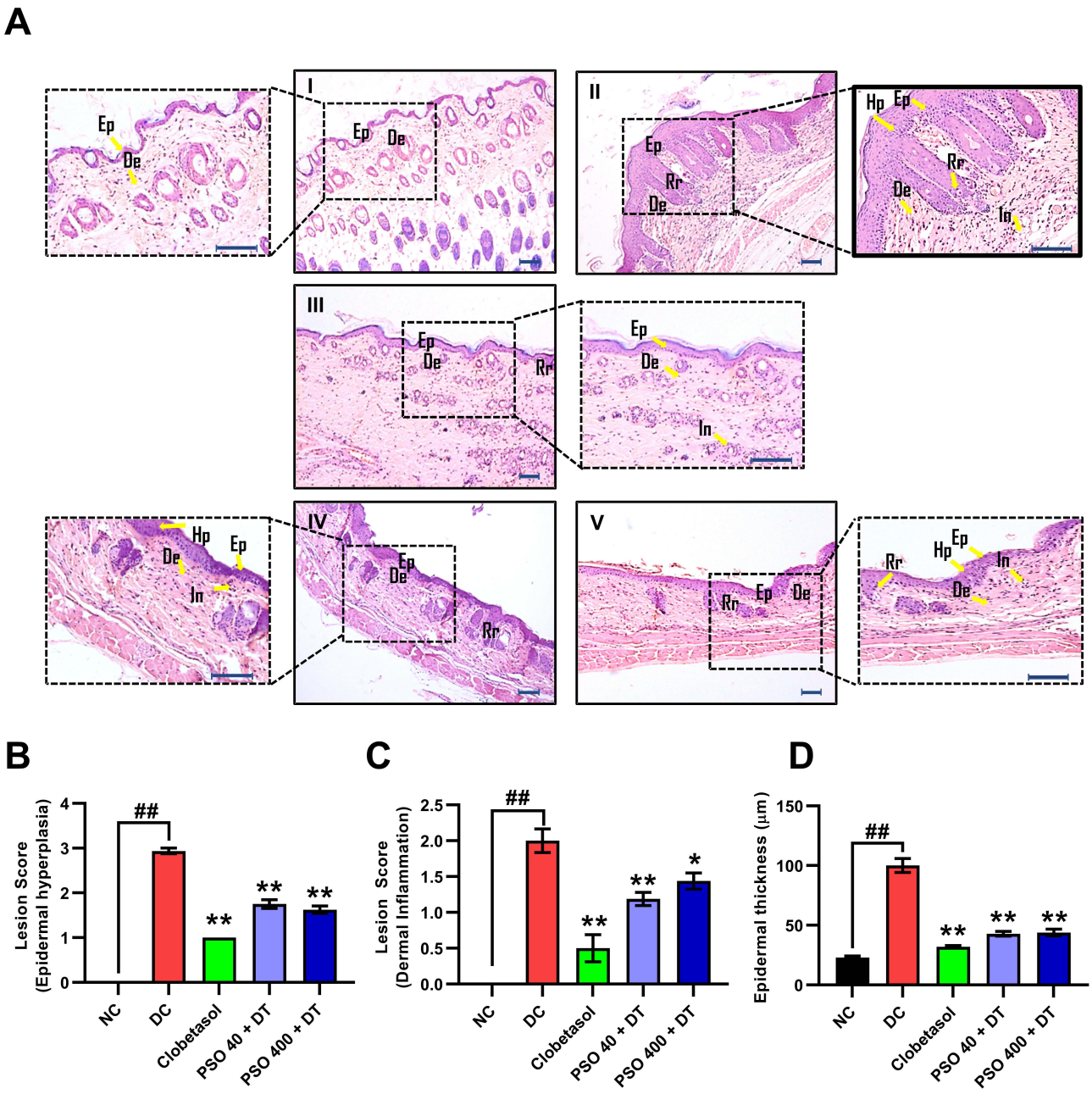

Figure 10 PSO and DT reversed histopathological changes and lesion scores of dorsal back skin in IMQ-induced psoriatic model. (**A**) Photomicrographs represent the histopathological analysis of dorsal back skin tissue performed following hematoxylin and eosin staining. Low-magnification images were obtained at 100X, and the higher-magnification image was obtained at 400X. (I) Normal control (NC) represents the normal epidermis (Ep), dermis (De), sebaceous gland (Sg), and cartilage (Ct). (II) Disease control (DC) represents hyperplastic epidermis (Hp), the presence of inflammatory cells (In) in the dermis region. (III) IMQ and Clobetasol treated dorsal back skin: the reduced hyperplastic epidermis (Ep), absence of inflammatory cells in the dermis region. (IV) IMQ and PSO 40 + DT (40 mpk/day PSO and 40 µL/day DT) treated ear: the reduced hyperplastic epidermis (Ep), the reduced presence of inflammatory cells (In) in the dermis region. (V) IMQ and PSO 400 + DT (400 mpk/day PSO and 40 µL/day DT) treated ear: the reduced hyperplastic epidermis (Ep). The scale represents 100 µm (n = 6–8 animals). Yellow arrows depict the specific cellular area of the skin tissue or the characteristic lesion. (**B** and **C**) The bar charts show lesion scores of hyperplasia of the epidermis and dermal inflammation. (**D**) The bar chart represents the effect of PSO and DT on reducing the epidermal thickness of ear skin. The data were analyzed by one-way ANOVA followed by Dunnett's multiple comparison tests. Statistical significance between NC and DC groups is represented as $^{\#\#}(p < 0.01)$ and between DC and PSO + DT groups (40 and 400 mpk/day) $^{*}(p < 0.05)$ or $^{**}(p < 0.01)$. The scale bar represents 100 µm.

In vivo Model 2: PSO and DT Attenuated TPA-Induced Ear Thickness

The combinatorial efficacy of PSO and DT was tested in the TPA-induced ear edema model. The topical application of TPA showed an increase in ear thickness in a time-dependent manner. The ear thicknesses from Day 1 reached a maximum on Day 5 and then almost remained inflamed and fairly constant till Day 11 (Figure 11A). The treatment

https://doi.org/10.2147/JIR.S505245

with PSO and DT showed a significant ($p < 0.01$) decrease in ear thickness from Day 5 onwards (Figure 11A). The data calculated based on the difference in ear thickness on Day 11 between different groups revealed that PSO and DT dose-dependently inhibited ear thickness. The percent inhibition data of PSO 40 + DT, PSO 120 + DT, and PSO 400 + DT doses showed inhibition of 74%, 76%, and 86% of the Δ ear thickness respectively (Figure 11B). The AUC (area under the curve) calculated for ear thickness from initiation of disease induction *ie* Day 1 up to termination of the experiment *ie* Day 11, PSO and DT showed to recover around 50% of the inflamed ears ($p < 0.01$) at all the tested doses (Figure 11C). The positive control group treated with clobetasol propionate showed inhibition of Δ ear thickness of 104% on Day 11 and around 97% inhibitions on AUC analysis (Figure 11B and C).

PSO and DT Reduced the TPA-Induced Ear Biopsy Weight

The ear biopsy weight taken on Day 11 revealed that TPA not only induced ear thickness but also significantly increased the weight of the ear in the tested animals (Figure 11D). The positive control group treated with clobetasol propionate demonstrated 82% inhibition of the TPA-induced increase in ear punch weight ($p < 0.01$). Similarly, the PSO 400 + DT treatment group was shown to significantly ($p < 0.05$) inhibit the TPA-induced increase in ear punch weight. The percent inhibition of 39%, 50%, and 70% of the ear weight was observed with the increasing dose of PSO and DT (Figure 11D).

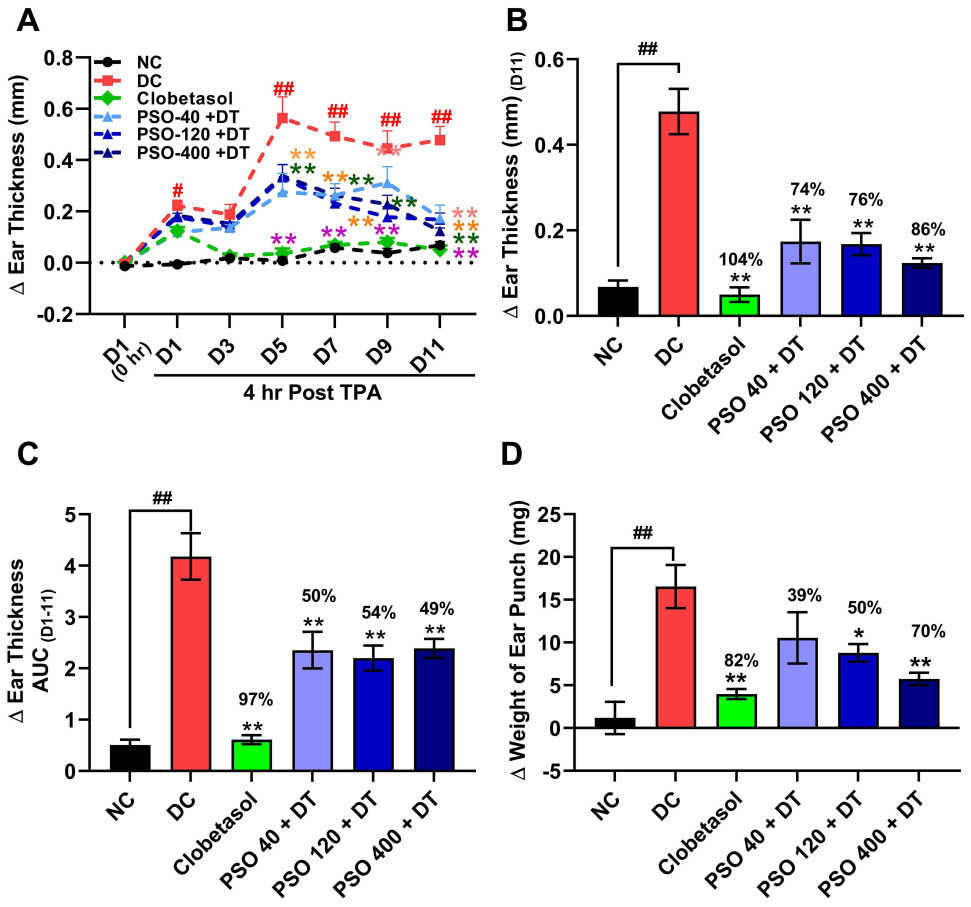

Figure 11 PSO and DT in combination reduced the TPA-induced ear edema model: (**A**) The line chart represents the effect of PSO and DT on Δ Ear Thickness from Day 1 to Day 11. (**B**) The bar chart shows the effect of PSO and DT on % inhibition of Δ Ear Thickness on Day 11. (**C**) The bar chart represents the effect of PSO and DT on the area under the curve (AUC) of Δ Ear Thickness from Day 1 to Day 11. (**D**) The bar chart represents the effect of PSO and DT on ear punch weight (mg). All values are represented as mean ± SEM, $n = 6–8$. Data were analyzed through two-way ANOVA followed by Tukey's multiple comparisons (Figure 11A) and one-way ANOVA followed by Dunnett's multiple comparison tests (Figure 11B-D). # and ## indicates significant difference with respect to NC (($p < 0.05$ and $p < 0.01$) whereas * and ** depict a statistically significant effect when compared to DC (*$p < 0.05$ and **$p < 0.01$).

PSO and DT Mitigated the TPA-Induced Histopathological Changes

Histopathological changes observed in the TPA-induced ear skin mimicked the structural changes observed in the psoriatic lesions as compared to the control (Figure 12A I). The majority of the hallmarks of psoriatic lesions such as epidermal hyperplasia, dermal inflammation, elongated rete ridges, and an increase in epidermal thickness were markedly observed in the ear sections of TPA-induced animals (Figure 12A II). Clobetasol propionate could also mitigate all the tested parameters in TPA-induced ear edema (Figure 12A III). In this study, the concurrent treatment of PSO and topical application of DT was shown to significantly reduce epidermal hyperplasia and rete ridge formation (Figure 12A IV and VI). In addition, the PSO and DT treatments also showed to inhibit the epidermal thickness significantly (Figure 12A IV and VI).

Upon lesion scoring through microscopic analysis of histopathological parameters of ear sections, PSO and DT were found to effectively reduce the psoriatic-like lesions in ear skin specimens. The scores revealed a significant difference in epidermal hyperplasia, dermal inflammation; elongated rete ridge formation, and epidermal thickness in TPA-induced diseased animals as compared to controls ($p < 0.01$). PSO at the doses of both 120 and 400 mpk/day + DT could significantly ($p < 0.01$) reduce epidermal hyperplasia (Figure 12B) whereas PSO+DT at all the tested doses (40, 120, and 400 mpk/day) was found to significantly mitigate the elongation of rete ridges in ear specimens ($p < 0.01$). Similar to histopathological data, lesion scores too could not find any efficacy of PSO and DT in mitigating dermal inflammation in TPA-challenged mice (Figure 12C and D). The total lesion score combining all the tested parameters such as epidermal hyperplasia, dermal inflammation, and rete ridge formation showed an overall scenario of PSO+DT, where PSO and DT in combination were found to effectively mitigate overall scoring of psoriatic lesions ($p < 0.01$) (Figure 12E). In addition, PSO at the dose of 400 mpk/day ($p < 0.01$) attenuated the aberrant epidermal thickening (Figure 12F). Similarly, the positive control group treated with clobetasol propionate was found to effectively mitigate ($p < 0.01$) all the tested psoriatic parameters in this experimental model (Figure 12B–F).

Discussion

Psoriasis affects both men and women of all age groups of different ethnic populations globally.[42] Most of the medications used in the treatment of psoriasis provide only symptomatic relief. These medications are laden with adverse effects such as tingling, numbness, headaches, and joint pain. A lacuna still persists in the long-term effective management of psoriasis. Natural products are being increasingly utilized for treatment of several inflammatory skin disorders like psoriasis.[43] The current study was designed to evaluate the efficacy of PSO, a polyherbal oral drug, and DT, an oil formulation for topical application, against psoriasis-like inflammatory skin diseases in both in vitro and in vivo studies. PSO is enriched with several important herbs and minerals known for remedial measures against skin-related diseases from ancient times. The UHPLC data revealed the presence of phytometabolites palmatine, β-ecdysone, berberine, protocatechuic acid, and rutin in PSO, which have broad anti-inflammatory and anti-psoriatic activities.[44] In addition, PSO was also found to contain gallic acid, magnoflorine, methyl gallate, cinnamic acid, and vanillic acid which are known to have antioxidant and anti-inflammatory activities.[45]

Pro-inflammatory mediators such as TNF-α, IL-12, IL-23, IL-17RA, and IL-17A are involved in the pathogenesis of psoriasis.[46,47] TNF-α contributes to the pathophysiology of psoriasis by inducing the gene expression of inflammatory cytokines, and also activate immune reactions. In recent years, anti-TNF-α therapeutic agents such as adalimumab, certolizumab pegol, etanercept, and infliximab have been approved for psoriasis.[48] In the current study, the anti-inflammatory efficacy of PSO was initially tested in TNF-α induced differentiated HaCaT (keratinocytes) cells. It was observed that PSO effectively mitigated TNF-α-induced chemokine release (IL-8) as well as the gene expression of pro-inflammatory mediators such as TNF-α, IL-8, and IL-1β in these cells. This might be due to the presence of rutin, a component of PSO, known to modulate the expression of genes such as IL-6, TNF-α, and IL-17 in in vitro and in vivo models of psoriasis.[49]

NF-κB is well-known for regulating the gene expression of several mediators involved in inflammation, cell survival, proliferation, and differentiation.[50] In this study, PSO treatment was found to down-regulate NF-κB activity in THP1-Blue NF-κB reporter cells. This anti-inflammatory effect of PSO might be attributed to the presence of phytometabolites such as palmatine, gallic acid, cinnamic acid, and methyl gallate which have anti-inflammatory activities.[51] Palmatine

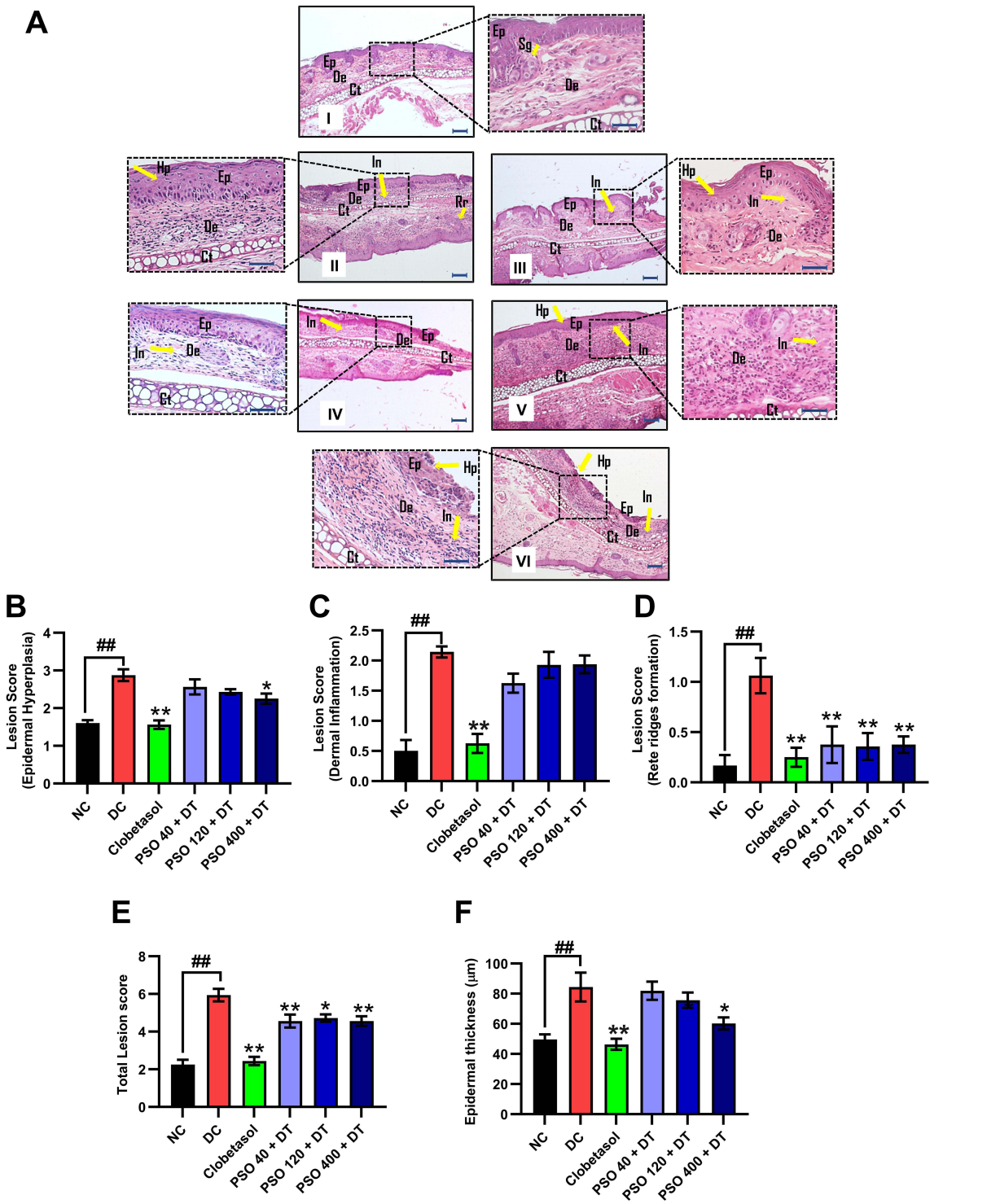

Figure 12 PSO and DT ameliorated the TPA-induced histopathological changes and the lesion scores in the ear edema model. (**A**) Photomicrographs represent the histopathological analysis of mice ear tissue through hematoxylin and eosin staining. Low-magnification images were obtained at 100X, and the higher-magnification images were obtained at 400X. (I) Normal control (NC) represents the normal epidermis (Ep), dermis (De), sebaceous gland (Sg), and cartilage (Ct). (II) Disease control (DC) represents hyperplastic epidermis (Hp), the presence of inflammatory cells (In) in the dermis region. (III) TPA and Clobetasol treated ear: the reduced hyperplastic epidermis (Ep), absence of inflammatory cells in the dermis region. (IV) TPA and PSO 40 + DT (40 mpk/day PSO and 40 µL/day DT) treated ear: the reduced hyperplastic epidermis (Ep), the reduced presence of inflammatory cells (In) in the dermis region. (V) TPA and PSO 120 + DT (120 mpk/day PSO and 40 µL/day DT) treated ear: the reduced hyperplastic epidermis (Ep). (**VI**) TPA and PSO 400 + DT (400 mpk/day. and 40 µL/day DT) treated ear: the reduced hyperplastic epidermis (Ep). The scale represents 100 µm (n = 6–8 animals). Yellow arrows depict the specific cellular area of the skin tissue or the characteristic lesion. (**B**–**E**) The bar charts represent lesion scores of epidermal hyperplasia, dermal inflammation, rete ridge formation of the epidermis, and the total lesion score of TPA-induced histopathological changes. (**F**) The bar chart represents epidermal thickness. All values are represented as mean ± SEM, n = 6–8. Data were analyzed through one-way ANOVA followed by Dunnett's multiple comparison test. $^{\#\#}$ indicates significant difference with respect to NC ($p < 0.01$) whereas * and ** depict a statistically significant effect when compared to DC (*$p < 0.05$ and **$p < 0.01$). The scale bar represents 100 µm.

originating from plants like *Tinospora cordifolia* (Giloy), *Berberis aristata* (Daruhaldi), and *Cyperus scariosus* (Nagarmotha) has previously been shown to decrease the IL-6 and TNF-α release in LPS-induced murine macrophages.[52] Moreover, palmatine has also been shown to mitigate monosodium-induced gouty arthritis by regulating NF-κB/NLRP3 and Nrf2 pathways.[53] Similarly, PSO-containing active molecules, such as cinnamic acid and methyl gallate, have also been found to regulate the NF-κB signaling mechanism.[54,55] Similarly, rutin was found to alleviate lupus-like symptoms in mice by inhibiting the release of cytokines, including TNF-α, IL-17, and IL-6 via modulation of NF-κB and STAT3[56] which also play a crucial role in psoriasis.[57]

IL-17/IL-23 axis plays a crucial role in the pathogenesis of psoriasis,[58] as also shown in in vivo model of IMQ-based psoriasis-like skin disorder.[59] IMQ is an immunomodulatory agent which is known to modulate the IL-17/IL-23 axis in psoriasis-like skin pathologies.[59–61] The use of IL-17/IL-23 pathway inhibitors suppresses inflammation and thereby mitigates the formation of psoriatic skin lesions.[62] In the present study, we evaluated PSO in the model of IMQ-induced psoriasis-like skin inflammation in differentiated HaCaT (keratinocytes) cells.[35] It was observed that PSO showed a reduction in the release of IL-17RA and the mRNA expression of IL-17RA and IL-23 in these cells.

IMQ predominantly acts via the TLR7 receptor of immune cells, leading to dermal inflammation, epidermal hyperplasia, and hyperkeratosis.[63–65] Thus, the combined effects of PSO and DT have been tested in the IMQ-induced psoriasis mice model. IMQ can also lead to systemic inflammation leading to enlargement of the spleen size.[39,66] Clobetasol which is used to provide relief for the symptomatic relief in psoriasis, has been utilized as a reference control in the current study. It is known to inhibit keratinocyte proliferation and has role in immunosuppression.[67] Clobetasol also has anti-inflammatory properties which could further contribute to a reduction in the keratosis and skin thickness, which are prominent markers of psoriasis.[68] Clobetasol exhibits its anti-inflammatory properties by inhibition of inflammatory cytokine release via interacting with cytosolic glucocorticoid receptors and by enhancing the mRNA expression of anti-inflammatory genes.[69,70]

In this study, we first evaluated the change in ear punch weight and spleen size upon IMQ application. It was observed that IMQ application led to both an increase in ear punch and relative spleen weight which were decreased upon combinatorial use of PSO and DT. Besides, PSO and DT in combination also mitigated histopathological changes, including epidermal hyperplasia, rete ridge formation, dermal inflammation, and epidermal thickness in both ear and back skin of the IMQ-induced psoriatic mice. Combined use of natural products is known to enhance anti-inflammatory potential of anti-psoriatic agents. A notable example of this would be the combined use of melatonin and rutin which showed a reduction in the levels of TNF-α and IL-17A as well as improvement in the histopathological aberrations in IMQ-induced psoriasis in mice model.[71]

Epidermal thickness is promoted by *KRT 17* via polarization of the immune cells at the site of the epidermis, leading to edema formation. Clinically, *KRT 17* levels were found to be positively correlated to psoriasis severity.[72] Hence, in this study, we analyzed the expression of *KRT 17* in the ear skin sample of IMQ-induced mice. An increase was observed in the mRNA expression of *KRT 17* in ear skin samples upon IMQ application. Treatment with PSO and DT normalized the expression of the *KRT 17* gene. This effect might be due to the presence of Gallic acid in PSO which is known to modulate *KRT 17* expression through Nrf2 regulation.[45] These potent effects of PSO might also be attributed to the presence of Ras Manikya in addition to different herbs. Ras Manikya is prepared by heating *Shuddha Haratala* (Arsenic trisulphide) sandwiched between *Abhrak Patra* (Mica).[73] Traditionally, Ras manikya has been used for various types of skin ailments, such as skin rashes, dry skin, eczema, leukoderma, and leprosy in the Indian subcontinent.[73] Additionally, phytometabolites from DT might also play a role in deterrence of the inflammatory pathophysiologies linked with psoriasis. Components like ar-turmerone, eucalyptol, and various fatty acids such as palmitic acid, palmitoleic acid, stearic acid, oleic acid, and linoleic acid present in DT contribute to its anti-psoriatic effects. ar-Turmerone has been known to possess anti-psoriatic activity in IMQ-induced mice model via regulation of NF-κB and MAPK pathway.[74] The topical application of fatty acids present in DT provides a soothing or moisturizing effect on the skin. These fatty acids predominantly originate from plants like *Curcuma longa* (Haldi), *Withania somnifera* (Ashwagandha), *Hippophae rhamnoides* (Seabuckthorn), *Berberis aristata, Azadirachta indica* (Neem), and *Sesamum indicum* (Sesame).[75] Hence, DT supports the hydration of skin during psoriasis.

To robustly establish the pharmacological benefits of PSO and DT, another model of TPA-induced ear edema (skin inflammation) was established.[76,77] The topical application of TPA onto the mice ear leads to the infiltration of neutrophils in the epidermis and dermis region and edema formation.[75,76] In this study, we found that the PSO and DT treatment reduced the ear thickness, ear punch weight, and psoriatic lesions. This effect of PSO might be attributed to the presence of β-ecdysone, a steroid hormone originating from plants like *Tinospora cordifolia* and *Berberis aristata*, which is known to attenuate the IL-1β-induced inflammatory signaling via modulation of NF-κB.[78] Berberine, another phytometabolite of PSO originating from *Berberis aristata*, has historically been utilized as an effective anti-inflammatory agent.[44] Many studies have shown its efficacy against inflammation via suppression of the JAK2/STAT3-mediated cellular signaling in skin cells.[79,80] Thus, the administration of PSO could decrease the TPA-induced ear inflammation, possibly through suppression of JAK2/STAT3 mediated inflammatory signaling. Additionally, compounds of PSO like rutin and protocatechuic acid present in PSO have previously been shown to have strong anti-oxidant and anti-inflammatory activity against different model systems of psoriasis.[81] In this study, the AUC calculated based on the increase in ear thickness from Day 1 till Day 11 in the TPA-induced ear edema model revealed an effective reduction of ear thickness in PSO and DT-treated animals. This correlates with previously reported studies on the anti-inflammatory effects of herbal formulations containing β-ecdysone, berberine, and protocatechuic acid.[78] Fatty acids like palmitic acid present in DT are known to resist the entry of harmful substances into the skin and aid in the maintenance of normal skin barrier function[75] thereby protecting further deterioration of psoriatic skin lesions.

This is the first report of the assessment of the pharmacological effects of Psorogrit and Divya-Taila in well-established models of psoriasis-like skin lesions. Based on the promising outcomes of the present study future experiments are necessary to evaluate the preclinical effectiveness of Psorogrit and Divya-Taila administrated concurrently with disease induction. Further, exploratory human trials involving Psorogrit and Divya-Taila will provide additional support to the present observation.

Conclusion

The polyherbal formulations, Psorogrit and Divya-Taila, in combination, showed anti-psoriatic activity in well-established in vitro and in vivo experimental models of psoriatic inflammation. This study suggests that Psorogrit and Divya-Taila could be used as therapeutic agents for psoriasis-like skin diseases.

Abbreviations

DT, Divya-Taila; *IL-1β*, *Interleukin 1 beta*; *IL-6*, *Interleukin 6*; *Interleukin 17A receptor*, *IL-17RA*, *Interleukin-23*, *IL-23*; IMQ, Imiquimod; *Keratin 17*, *KRT 17*; NF-κB Nuclear factor kappa-light-chain-enhancer of activated B cells; PSO, Psorogrit; ROS, Reactive oxygen species; TNF-α, Tumour Necrosis Factor-alpha; TPA 12-O-tetradecanoylphorbol-13-Acetate.

Data Sharing Statement

The original contributions presented in the study are included in the article; further inquiries can be directed to the corresponding author.

Ethical Approval and Consent to Participate

The animal study was reviewed and approved by the Institutional Animal Ethics Committee (IAEC) of Patanjali Research Foundation as per the approval numbers PRIAS/LAF/IAEC-125 and PRIAS/LAF/IAEC-126.

Acknowledgments

The authors extend their gratitude to Ms. Deepika Rajput and Ms. Deepika Mehra for their support in the biochemical analysis. In addition, the authors are grateful to Mr. Yash Varshney, Dr. Seema Gujral, and Dr. Jyotish Srivastava for their help in phytochemical analysis. We also appreciate Mr. Mir Chand, Mr. Ram Hari Sharma, Mr. Pushpender Singh, and Mr. Sonit Kumar for their support in animal handling and maintenance. We acknowledge Dr. Vivek Gohel for experiments pertaining to IMQ-induced keratinocytes and his noteworthy comments regarding the manuscript. The authors extend their

gratitude to Mr. Devendra Kumawat for his excellent graphical representations for the manuscript. The authors are also grateful to Ms. Simran Gera, Mr. Tarun Rajput and Mr. Gagan Kumar for their swift administrative support.

Author Contributions

All authors made a significant contribution to the work reported, whether that is in the conception, study design, execution, acquisition of data, analysis and interpretation, or in all these areas; took part in drafting, revising or critically reviewing the article; gave final approval of the version to be published; have agreed on the journal to which the article has been submitted; and agree to be accountable for all aspects of the work.

Funding

Patanjali Research Foundation Trust, Haridwar, India funded this research work internally.

Disclosure

The test articles (Psorogrit and Divya-Taila) were sourced from Divya Pharmacy, Haridwar, Uttarakhand, India. Acharya Balkrishna is an honorary trustee in Divya Yog Mandir Trust, which governs Divya Pharmacy, Haridwar. In addition, he holds an honorary managerial position in Patanjali Ayurved Ltd, Haridwar, India. Other than providing the test formulations (Psorogrit and Divya-Taila), Divya Pharmacy was not involved in any aspect of the research reported in this study. The remaining authors declare no potential conflict of interest.

References

1. Jiang Y, Tsoi LC, Billi AC, et al. Cytokinocytes: the diverse contribution of keratinocytes to immune responses in skin. *J JCI Insight*. 2020;5(20).
2. Lowes MA, Suarez-Farinas M, Krueger JG. Immunology of psoriasis. *Annu Rev Immunol*. 2014;32(1):227–255. doi:10.1146/annurev-immunol-032713-120225
3. WHO. Global report on psoriasis. In: World Health Organization Geneva; 2016.
4. Parisi R, Symmons DP, Griffiths CE, Ashcroft DM. Global epidemiology of psoriasis: a systematic review of incidence and prevalence. *J Investig Dermatol*. 2013;133(2):377–385. doi:10.1038/jid.2012.339
5. AlShobaili HA, Shahzad M, Al-Marshood A, Khalil A, Settin A, Barrimah I. Genetic background of psoriasis. *Int J Health Sci*. 2010;4(1):23.
6. Bugaut H, Aractingi S. Major role of the IL17/23 axis in psoriasis supports the development of new targeted therapies. *Front Immunol*. 2021;12:621956. doi:10.3389/fimmu.2021.621956
7. Mavropoulos A, Rigopoulou EI, Liaskos C, Bogdanos DP, Sakkas LI. The role of p38 MAPK in the aetiopathogenesis of psoriasis and psoriatic arthritis. *J Immunol Res*. 2013;2013(1):569751.
8. Id BA. T-helper 17 cells in psoriatic plaques and additional genetic links between IL-23 and psoriasis. *J Invest Dermatol*2008;128(5):1064–1067.
9. Koga C, Kabashima K, Shiraishi N, Kobayashi M, Tokura YJJo ID. Possible pathogenic role of Th17 cells for atopic dermatitis. *J Invest Dermatol*. 2008;128(11):2625–2630. doi:10.1038/jid.2008.111
10. Albanesi C, Scarponi C, Cavani A, Federici M, Nasorri F, GJJoid G. Interleukin-17 is produced by both Th1 and Th2 lymphocytes, and modulates interferon-γ-and interleukin-4-induced activation of human keratinocytes. *J Invest Dermatol*. 2000;115(1):81–87. doi:10.1046/j.1523-1747.2000.00041.x
11. Di Cesare A, Di Meglio P, Nestle FOJJo ID. The IL-23/Th17 axis in the immunopathogenesis of psoriasis. *J Invest Dermatol*. 2009;129(6):1339–1350. doi:10.1038/jid.2009.59
12. SC-S H, Lan -C-CE. Psoriasis and cardiovascular comorbidities: focusing on severe vascular events, cardiovascular risk factors and implications for treatment. *Int J mol Sci*. 2017;18(10):2211. doi:10.3390/ijms18102211
13. De Francesco MA, Caruso A. The gut microbiome in psoriasis and crohn's disease: is its perturbation a common denominator for their pathogenesis? *J Vaccines*. 2022;10(2):244.
14. Fotiadou C, Lazaridou E. Therapy psoriasis and uveitis: links and risks. *J Psoriasis*. 2019;91–96.
15. Uva L, Miguel D, Pinheiro C, et al. Mechanisms of action of topical corticosteroids in psoriasis. *Int J Endocrinol*. 2012;2012(1):561018. doi:10.1155/2012/561018
16. Kim GK. The rationale behind topical vitamin d analogs in the treatment of psoriasis: where does topical calcitriol fit in? *JCAD*. 2010;3(8):46.
17. Warren E, Khanderia U. Use of retinoids in the treatment of psoriasis. *J Clin Pharmacol*. 1989;8(5):344–351.
18. Dattola A, Silvestri M, Bennardo L, et al. Update of calcineurin inhibitors to treat inverse psoriasis: a systematic review. *Dermatol Ther*. 2018;31(6):e12728. doi:10.1111/dth.12728
19. Xie J, Huang S, Huang H, et al. Advances in the application of natural products and the novel drug delivery systems for psoriasis. *Front. pharmacol*. 2021;12:644952. doi:10.3389/fphar.2021.644952
20. Rosso JQJTJoc D, Dermatology a. Topical corticosteroid therapy for psoriasis—a review of clobetasol propionate 0.025% cream and the clinical relevance of penetration modification. *J Clin Aesthet Dermatol*. 2020;13(2):22.
21. Al-Jabr KH, Alhumaidan LS, Alghamdi AA, et al. Awareness of side effects of corticosteroids among users and nonusers in Saudi Arabia. *J Pharm Pharmacol* . 2024;16(Suppl 2):S1612–S1618. doi:10.4103/jpbs.jpbs_925_23
22. Hawkes JE, Yan BY, Chan TC, Krueger JGJTJo I. Discovery of the IL-23/IL-17 signaling pathway and the treatment of psoriasis. *J Immunol*. 2018;201(6):1605–1613. doi:10.4049/jimmunol.1800013

23. Armstrong AW, Read CJJ. Pathophysiology, clinical presentation, and treatment of psoriasis: a review. *JAMA*. 2020;323(19):1945–1960. doi:10.1001/jama.2020.4006
24. Puig L. Induction phase, primary endpoint, time to decide on primary failure, and therapeutic goals in biologic treatment of psoriasis. *J. Eur. Acad. Dermatol. Venereol*. 2013. 27(2).
25. Porter C, Woods A, Mendelow M, Purvis C, SJJoDi F. *Unmet Needs Psoriasis Patients*. 2022;21(8):839–844.
26. Lim D-W, Kim H, Kim Y-M, Chin Y-W, Park W-H, Kim J-E. Drug repurposing in alternative medicine: herbal digestive sochehwan exerts multifaceted effects against metabolic syndrome. *Sci Rep*. 2019;9(1):9055. doi:10.1038/s41598-019-45099-x
27. Elkhawaga OY, Ellety MM, Mofty SO, Ghanem MS, Mohamed AO. Review of natural compounds for potential psoriasis treatment. *Inflammopharmacology*. 2023;31(3):1183–1198. doi:10.1007/s10787-023-01178-0
28. Balkrishna A, Gohel V, Pathak N, et al. Anti-oxidant response of lipidom modulates lipid metabolism in Caenorhabditis elegans and in OxLDL-induced human macrophages by tuning inflammatory mediators. *Biomed Pharmacother*. 2023;160:114309. doi:10.1016/j.biopha.2023.114309
29. Balkrishna A, Gohel V, Pathak N, et al. Anti-hyperglycemic contours of madhugrit are robustly translated in the *Caenorhabditis elegans* model of lipid accumulation by regulating oxidative stress and inflammatory response. *Front Endocrinol*. 2022;13:1064532. doi:10.3389/fendo.2022.1064532
30. Balkrishna A, Gohel V, Singh R, Bhattacharya K, Varshney A. Livogrit ameliorates acetaldehyde-induced steatosis in HepG2 cells through modulation of lipogenesis and β-oxidation pathways. *Phytomedicine Plus*. 2021;1(3):100067. doi:10.1016/j.phyplu.2021.100067
31. Rizvi DA, Fatima Z, Kaur CD. Antipsoriatic and anti-inflammatory studies of *Berberis aristata* extract loaded nanovesicular gels. *J Pharmacognosy Magazine*. 2017;13(Suppl 3):S587.
32. Gęgotek A, Jastrząb A, Jarocka-Karpowicz I, Muszyńska M, Skrzydlewska E. The effect of sea buckthorn (*Hippophae rhamnoides* L.) seed oil on UV-induced changes in lipid metabolism of human skin cells. *J Antioxidants*. 2018;7(9):110. doi:10.3390/antiox7090110
33. Baby AR, Freire TB, GdA M, et al. *Azadirachta indica* (Neem) as a potential natural active for dermocosmetic and topical products: a narrative review. *J Cosmetics*. 2022;9(3):58.
34. Balkrishna A, Nain P, Chauhan A, et al. Super critical fluid extracted fatty acids from *Withania somnifera* seeds repair psoriasis-like skin lesions and attenuate pro-inflammatory cytokines (TNF-α and IL-6) release. *J Biomolecules*. 2020;10(2):185.
35. Varma SR, Sivaprakasam TO, Mishra A, Prabhu S, Rafiq M, Rangesh P. Imiquimod-induced psoriasis-like inflammation in differentiated human keratinocytes: its evaluation using curcumin. *Eur J Pharmacol*. 2017;813:33–41. doi:10.1016/j.ejphar.2017.07.040
36. du Sert NP, Hurst V, Ahluwalia A, et al. The ARRIVE guidelines 2.0: updated guidelines for reporting animal research. *JCBFM*. 2020;40(9):1769–1777.
37. Nair AB, Jacob S. A simple practice guide for dose conversion between animals and human. *JBCP*. 2016;7(2):27. doi:10.4103/0976-0105.177703
38. Sato K, Takaishi M, Tokuoka S, Sano S. Involvement of TNF-α converting enzyme in the development of psoriasis-like lesions in a mouse model. *J PLoS One*. 2014;9(11):e112408. doi:10.1371/journal.pone.0112408
39. Kim CH, Lee J, Yoo J, et al. Inhibitory effect of imiquimod-induced psoriasis-like skin inflammation in mice by histamine H4 receptor agonist 4-methylhistamine. *Scand J Immunol*. 2016;83(6):409–417. doi:10.1111/sji.12420
40. Shinno-Hashimoto H, Eguchi A, Sakamoto A, et al. Effects of splenectomy on skin inflammation and psoriasis-like phenotype of imiquimod-treated mice. *J Sci Rep*. 2022;12(1):14738. doi:10.1038/s41598-022-18900-7
41. Zhou X, Chen Y, Cui L, Shi Y, Guo C. Advances in the pathogenesis of psoriasis: from keratinocyte perspective. *CDD*. 2022;13(1):81.
42. Danielsen K, Olsen A, Wilsgaard T, Furberg AS. Is the prevalence of psoriasis increasing? A 30-year follow-up of a population-based cohort. *Br J Dermatol*. 2013;168(6):1303–1310. doi:10.1111/bjd.12230
43. Balkrishna A, Sakat SS, Joshi K, et al. Cytokines driven anti-inflammatory and anti-psoriasis like efficacies of nutraceutical sea buckthorn (*Hippophae rhamnoides*) oil. *Front Pharmacol*. 2019;10:1186. doi:10.3389/fphar.2019.01186
44. Yasukawa K, Takido M, Ikekawa T, Shimada F, Takeuchi M, Nakagawa S. Relative inhibitory activity of berberine-type alkaloids against 12-O-tetradecanoylphorbol-13-acetate-induced inflammation in mice. *Chem Pharm Bull*. 1991;39(6):1462–1465. doi:10.1248/cpb.39.1462
45. Zhang J, Li X, Chen H, et al. Gallic acid inhibits the expression of keratin 16 and keratin 17 through Nrf2 in psoriasis-like skin disease. *Int Immunopharmacol*. 2018;65:84–95. doi:10.1016/j.intimp.2018.09.048
46. Metko D, Torres T, Imr VR. Viewpoint about biologic agents for psoriasis: are they immunosuppressants or immunomodulators? *J Int Med Res*. 2023;51(6):03000605231175547. doi:10.1177/03000605231175547
47. Ruggiero A, Picone V, Martora F, Fabbrocini G, Guselkumab MM. Risankizumab, and tildrakizumab in the management of psoriasis: a review of the real-world evidence. *Clin Cosmet Invest Dermatol*. 2022;15:1649–1658. doi:10.2147/CCID.S364640
48. Griffiths CE, Armstrong AW, Gudjonsson JE, Barker JN. Psoriasis. *Lancet*. 2021;397(10281):1301–1315. doi:10.1016/S0140-6736(20)32549-6
49. Wang M, Ma X, Gao C, et al. Rutin attenuates inflammation by downregulating AGE-RAGE signaling pathway in psoriasis: network pharmacology analysis and experimental evidence. *Int Immunopharmacol*. 2023;125:111033. doi:10.1016/j.intimp.2023.111033
50. Liu T, Zhang L, Joo D, Sun S-C. NF-κB signaling in inflammation. *Signal Transduct Target Ther*. 2017;2(1):1–9.
51. Singh S, Singh TG, Mahajan K, Dhiman S. Pharmacology medicinal plants used against various inflammatory biomarkers for the management of rheumatoid arthritis. *J Pharm*. 2020;72(10):1306–1327. doi:10.1111/jphp.13326
52. Chen G, Xu Y, Jing J, et al. The anti-sepsis activity of the components of huanglian jiedu decoction with high lipid A-binding affinity. *Int Immunopharmacol*. 2017;46:87–96. doi:10.1016/j.intimp.2017.02.025
53. Cheng -J-J, Ma X-D, Ai G-X, et al. Palmatine protects against MSU-induced gouty arthritis via regulating the NF-κB/NLRP3 and Nrf2 pathways. *Drug Des Dev*. 2023;2119–2132.
54. Correa LB, Seito LN, Manchope MF, et al. Methyl gallate attenuates inflammation induced by toll-like receptor ligands by inhibiting MAPK and NF-Kb signaling pathways. *J Inflamm Res*. 2020;69:1257–1270. doi:10.1007/s00011-020-01407-0
55. Ibrahim EA, Moawed FS, Moustafa EM. Suppression of inflammatory cascades via novel cinnamic acid nanoparticles in acute hepatitis rat model. *Arch Biochem Biophys*. 2020;696:108658. doi:10.1016/j.abb.2020.108658
56. Yi T, Zhang W, Hua Y, et al. Rutin alleviates lupus nephritis by inhibiting T cell oxidative stress through PPARγ. *Chem. -Biol. Interact*. 2024;394:110972. doi:10.1016/j.cbi.2024.110972

57. Guo J, Zhang H, Lin W, et al. Signaling pathways and targeted therapies for psoriasis. *Signal Transduct. Target. Ther.* 2023;8(1):437. doi:10.1038/s41392-023-01655-6
58. Burakoff R, Barish CF, Riff D, et al. A Phase 1/2A trial of STA 5326, an oral interleukin-12/23 inhibitor, in patients with active moderate to severe Crohn's disease. *Inflamm. Bowel Dis*. 2006;12(7):558–565. doi:10.1097/01.ibd.0000225337.14356.31
59. Der Fits L V, Mourits S, Voerman JS, et al. Imiquimod-induced psoriasis-like skin inflammation in mice is mediated via the IL-23/IL-17 axis. *J Immun*. 2009;182(9):5836–5845. doi:10.4049/jimmunol.0802999
60. El Malki K, Karbach SH, Huppert J, et al. An alternative pathway of imiquimod-induced psoriasis-like skin inflammation in the absence of interleukin-17 receptor a signaling. *J Invest Dermatol*. 2013;133(2):441–451. doi:10.1038/jid.2012.318
61. Ridha-Salman H, Al-Zubaidy AA, Abbas AH, Hassan DM, SAJN-SsAo M. The alleviative effects of canagliflozin on imiquimod-induced mouse model of psoriasis-like inflammation. 2024;1–21.
62. Blauvelt A, Kimball AB, Augustin M, et al. Efficacy and safety of mirikizumab in psoriasis: results from a 52-week, double-blind, placebo-controlled, randomized withdrawal. *Br J Dermatol*. 2022;187(6):866–877. doi:10.1111/bjd.21743
63. Gilliet M, Conrad C, Geiges M, et al. Psoriasis triggered by toll-like receptor 7 agonist imiquimod in the presence of dermal plasmacytoid dendritic cell precursors. *Arch Dermatol*. 2004;140(12):1490–1495. doi:10.1001/archderm.140.12.1490
64. Almudaris SA, Fkjp G. Effects of topical ivermectin on imiquimod-induced psoriasis in mouse model–novel findings. *Pharmacia*. 2024;71:1–14.
65. Ridha-Salman H, Shihab EM, Hasan HK, et al. Mitigative effects of topical norfloxacin on an imiquimod-induced murine model of psoriasis. *ACS Pharmacology &amp*. 2024;7(9):2739–2754. doi:10.1021/acsptsci.4c00152
66. Moos S, Mohebiany AN, Waisman A, Kurschus FCJJo ID. Imiquimod-induced psoriasis in mice depends on the IL-17 signaling of keratinocytes. *J Invest Dermatol*. 2019;139(5):1110–1117. doi:10.1016/j.jid.2019.01.006
67. Salman HR, Alzubaidy AA, Abbas AH, Tums MH. Attenuated effects of topical vinpocetine in an imiquimod-induced mouse model of psoriasis. *J. Taibah Univ. Med. Sci*. 2024;19(1):35–53.
68. Heim M, Irondelle M, Duteil L, et al. Impact of topical emollient, steroids alone or combined with calcipotriol, on the immune infiltrate and clinical outcome in psoriasis. *Exp Dermatol*. 2022;31(11):1764–1778. doi:10.1111/exd.14657
69. Feldman SR, BAJAjocd Y. Topical clobetasol propionate in the treatment of psoriasis: a review of newer formulations. *Am J Clin Dermatol*. 2009;10(6):397–406. doi:10.2165/11311020-000000000-00000
70. Khafaji AWM, Al-Zubaidy AAK, Farhood IG, HRJN-SsAo S. Ameliorative effects of topical ramelteon on imiquimod-induced psoriasiform inflammation in mice. 2024;1–18.
71. Khorsheed SM, Abu-Raghif AR, Ridha-Salman HJP. Alleviative effects of combined topical melatonin and rutin on imiquimod-induced psoriasis mouse model. 2024;71:1–13.
72. Jin L, Wang G. Keratin 17: a critical player in the pathogenesis of psoriasis. *Med Res Rev*. 2014;34(2):438–454. doi:10.1002/med.21291
73. Shivhare V, Tiwari N. Therapeutics ayurveda perspective of rasamanikya and its role in skin disorders: a review. *J Drug Deliv*. 2019;9(6–s):267–269.
74. Li Y-L, Du Z-Y, Li P-H, et al. Aromatic-turmerone ameliorates imiquimod-induced psoriasis-like inflammation of BALB/c mice. *Int Immunopharmacol*. 2018;64:319–325. doi:10.1016/j.intimp.2018.09.015
75. Yang M, Zhou M, Song L. A review of fatty acids influencing skin condition. *J Cosmet Dermatol*. 2020;19(12):3199–3204. doi:10.1111/jocd.13616
76. Bhaskarmurthy DH, Prince SE. Effect of baricitinib on TPA-induced psoriasis like skin inflammation. *J Life Sci*. 2021;279:119655. doi:10.1016/j.lfs.2021.119655
77. Madsen M, Hansen PR, Nielsen LB, et al. Effect of 12-O-tetradecanoylphorbol-13-acetate-induced psoriasis-like skin lesions on systemic inflammation and atherosclerosis in hypercholesterolaemic apolipoprotein E deficient mice. *J BMC Dermatology*. 2016;16:1–10.
78. Zhang X, Xu X, Xu T, Qin S. β-Ecdysterone suppresses interleukin-1β-induced apoptosis and inflammation in rat chondrocytes via inhibition of NF-κB signaling pathway. *Drug Dev Res*. 2014;75(3):195–201. doi:10.1002/ddr.21170
79. Li M, Qin Z, Yu Q, et al. Anti-inflammatory activation of phellodendri chinensis cortex is mediated by berberine erythrocytes self-assembly targeted delivery system. *Drug Des Devel Ther*. 2022:4365–4383.
80. Zhu K, Yao Y, Wang K, et al. Berberin sustained-release nanoparticles were enriched in infarcted rat myocardium and resolved inflammation. *J Nanobiotechnology*. 2023;21(1):33. doi:10.1186/s12951-023-01790-w
81. Lee SH, Choi BY, Kho AR, et al. Protective effects of protocatechuic acid on seizure-induced neuronal death. *Int J mol Sci*. 2018;19(1):187. doi:10.3390/ijms19010187